

(19) **United States**

(12) **Patent Application Publication**
NAKAHATA et al.

(10) **Pub. No.: US 2021/0005364 A1**

(43) **Pub. Date: Jan. 7, 2021**

(54) **MAGNETIC CORE, METHOD OF
MANUFACTURING SAME, AND COIL
COMPONENT**

(71) Applicant: **TDK CORPORATION**, Tokyo (JP)

(72) Inventors: **Isao NAKAHATA**, Tokyo (JP);
Kazuhiro YOSHIDOME, Tokyo (JP);
Hirofumi MATSUMOTO, Tokyo (JP);
Akito HASEGAWA, Tokyo (JP)

(73) Assignee: **TDK CORPORATION**, Tokyo (JP)

(21) Appl. No.: **16/977,738**

(22) PCT Filed: **Mar. 1, 2019**

(86) PCT No.: **PCT/JP2019/008126**

§ 371 (c)(1),

(2) Date: **Sep. 2, 2020**

(30) **Foreign Application Priority Data**

Mar. 2, 2018 (JP) 2018-037526
Aug. 27, 2018 (JP) 2018-158585

Publication Classification

(51) **Int. Cl.**

H01F 1/153 (2006.01)

H01F 41/02 (2006.01)

H01F 27/25 (2006.01)

(52) **U.S. Cl.**

CPC **H01F 1/15308** (2013.01); **H01F 27/25**
(2013.01); **H01F 41/0226** (2013.01); **H01F**
1/15333 (2013.01)

(57)

ABSTRACT

A magnetic core and the like having a stable soft magnetic property, including a plurality of soft magnetic layers which are laminated, wherein a crack is formed in the soft magnetic layers. The soft magnetic layers include Fe as a principal component. The soft magnetic layers include a composition formula $(\text{Fe}_{(1-(\alpha+\beta))}\text{X1}_\alpha\text{X2}_\beta)_{(1-(a+b+c+d+e+f))}\text{M}_a\text{B}_b\text{P}_c\text{Si}_d\text{C}_e\text{S}_f$ wherein: X1 is one or more selected from the group consisting of Co and Ni, X2 is one or more selected from the group consisting of Al, Mn, Ag, Zn, Sn, As, Sb, Cu, Cr, Bi, N, and O and rare-earth elements, M is one or more selected from the group consisting of Nb, Hf, Zr, Ta, Mo, V, and W; and a to f and α and β are in predetermined ranges. A structure including a nanoheterostructure or an Fe-group nanocrystal is observed in the soft magnetic layers.

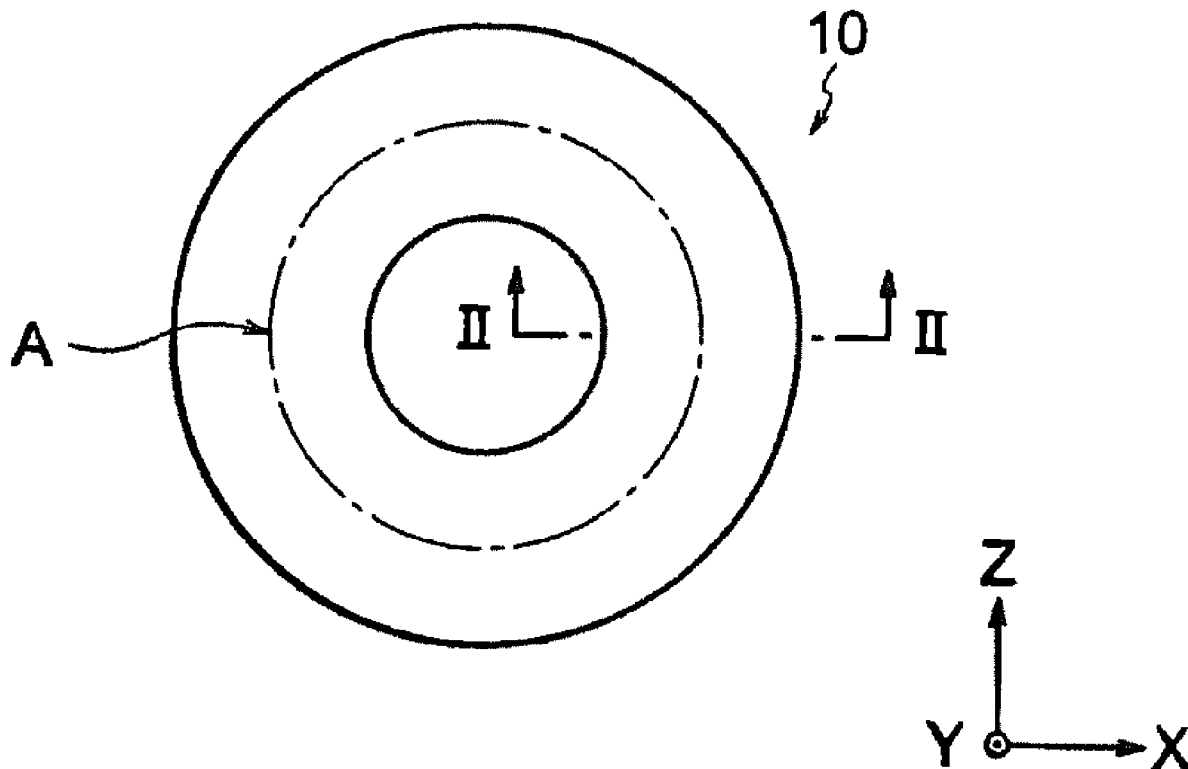


FIG. 1

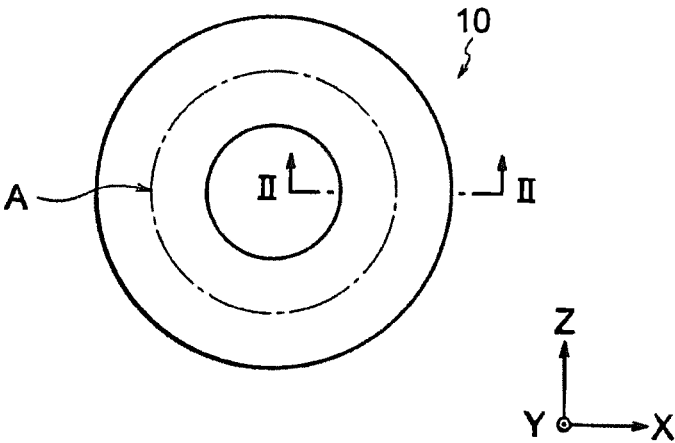


FIG. 2

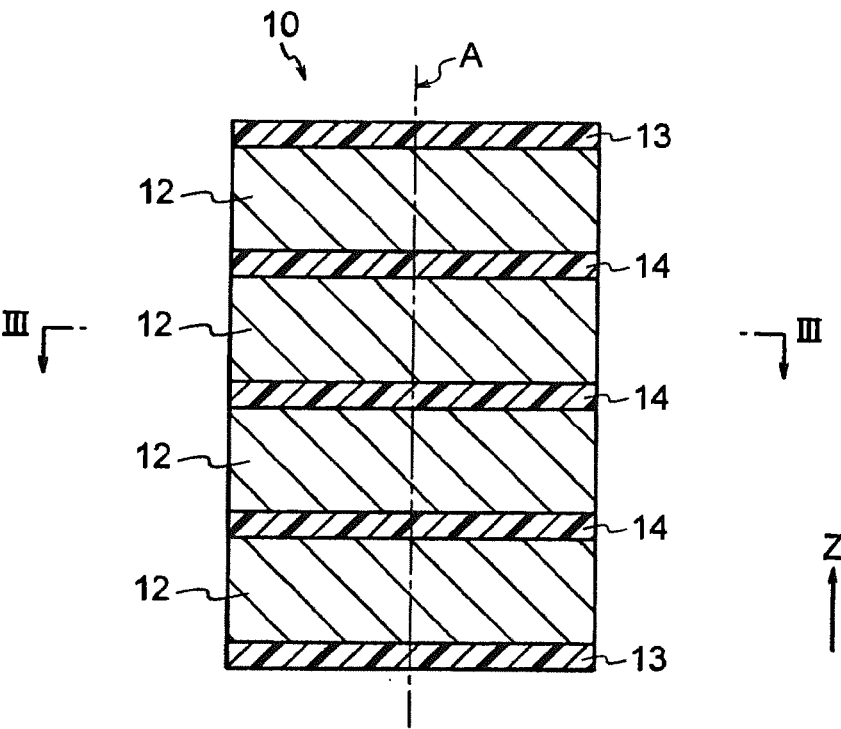


FIG. 3

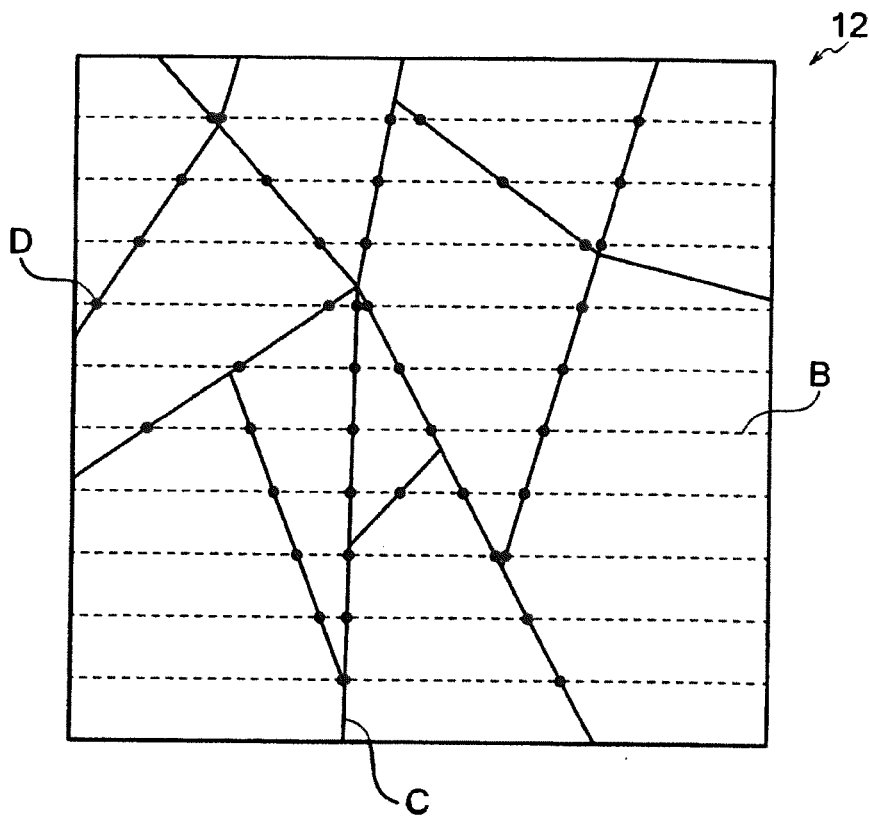


FIG. 4

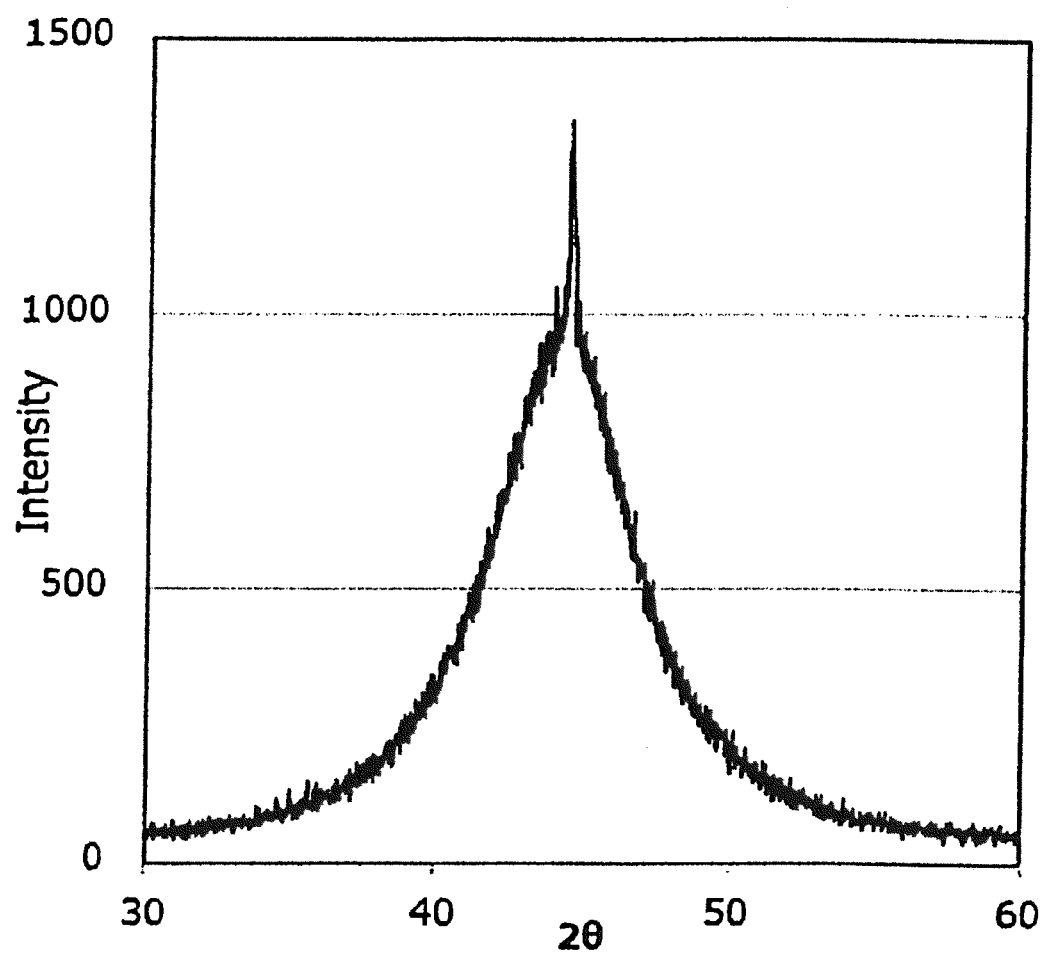
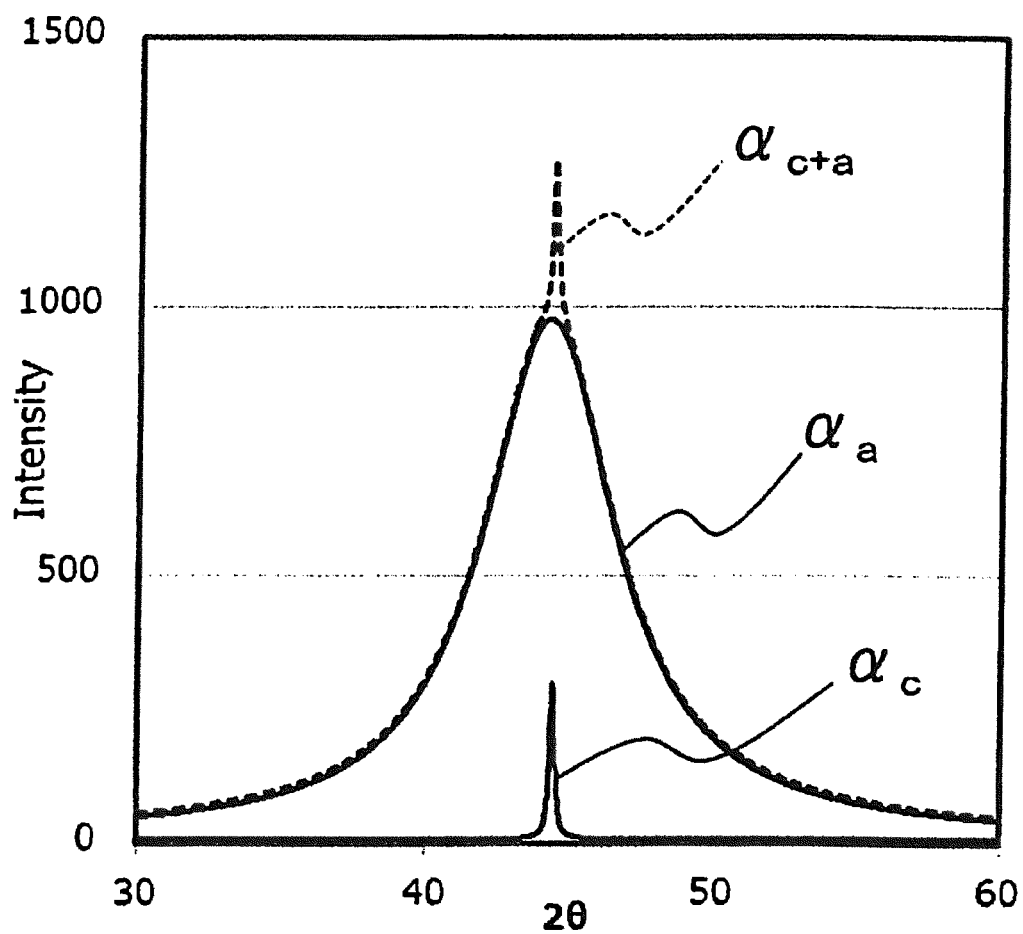


FIG. 5



MAGNETIC CORE, METHOD OF MANUFACTURING SAME, AND COIL COMPONENT

FIELD OF THE INVENTION

[0001] The present invention relates to a magnetic core, a method of manufacturing the magnetic core, and a coil device.

RELATED ART

[0002] In accordance with the recent miniaturization of power devices, further miniaturization of transformers and coils, which occupy a lot of space in the power devices, is desired. Patent Document 1 discloses that a metal soft magnetic material is used as a material of a magnetic core for transformers and coils. Moreover, forming a magnetic core by lamination is studied.

[0003] When the magnetic core is formed by lamination with a soft magnetic metal material as the magnetic material, however, there is a problem with difficulty in punching due to hardness of the metal soft magnetic material itself and with deterioration in soft magnetic characteristics (particularly, increase in coercivity) due to the stress applied at the time of punching.

PRIOR ART

Patent Document

[0004] Patent Document 1: JPH1174108 (A)

SUMMARY OF THE INVENTION

Problem to be Solved by the Invention

[0005] The present invention has been achieved under the circumstances. It is an object of the invention to provide a magnetic core etc. having stable soft magnetic characteristics.

Means for Solving the Problem

[0006] To achieve the above object, a magnetic core according to the first aspect of the present invention includes laminated soft magnetic layers having cracks, wherein

[0007] the soft magnetic layers include Fe as a main component,

[0008] the soft magnetic layers have a composition formula of $(\text{Fe}_{(1-(\alpha+\beta))}\text{X1}_\alpha\text{X2}_\beta)_{(1-(a+b+c+d+e+f))}\text{M}_d\text{B}_b\text{P}_c\text{Si}_d\text{C}_e\text{S}_f$ in which X1 is one or more selected from a group consisting of Co and Ni, X2 is one or more selected from a group consisting of Al, Mn, Ag, Zn, Sn, As, Sb, Cu, Cr, Bi, N, O, and rare earth elements, and M is one or more selected from a group consisting of Nb, Hf, Zr, Ta, Mo, V, and W, [0009] $0 \leq a \leq 0.140$, $0.020 < b \leq 0.200$, $0 \leq c \leq 0.150$, $0 \leq d \leq 0.180$, $0 \leq e < 0.040$, $0 \leq f \leq 0.030$, $\alpha \geq 0$, $\beta \geq 0$, and $0 \leq \alpha + \beta \leq 0.50$ are satisfied,

[0010] one or more of a, c, and d are larger than zero, and

[0011] a nanohetero structure including an amorphous phase and fine crystals existing in the amorphous phase is observed in the soft magnetic layers.

[0012] The fine crystals may have an average grain size of 0.3-5 nm.

[0013] A magnetic core according to the second aspect of the present invention includes laminated soft magnetic layers having cracks, wherein

[0014] the soft magnetic layers include Fe as a main component,

[0015] the soft magnetic layers have a composition formula of $(\text{Fe}_{(1-(\alpha+\beta))}\text{X1}_\alpha\text{X2}_\beta)_{(1-(a+b+c+d+e+f))}\text{M}_d\text{B}_b\text{P}_c\text{Si}_d\text{C}_e\text{S}_f$ in which X1 is one or more selected from a group consisting of Co and Ni, X2 is one or more selected from a group consisting of Al, Mn, Ag, Zn, Sn, As, Sb, Cu, Cr, Bi, N, O, and rare earth elements, and M is one or more selected from a group consisting of Nb, Hf, Zr, Ta, Mo, V, and W,

[0016] $0 \leq a \leq 0.140$, $0.020 < b \leq 0.200$, $0 \leq c \leq 0.150$, $0 \leq d \leq 0.180$, $0 \leq e < 0.040$, $0 \leq f \leq 0.030$, $\alpha \geq 0$, $\beta \geq 0$, and $0 \leq \alpha + \beta \leq 0.50$ are satisfied,

[0017] one or more of a, c, and d are larger than zero, and

[0018] a structure including Fe based nanocrystals is observed in the soft magnetic layers.

[0019] The Fe based nanocrystals may have an average grain size of 5-30 nm.

[0020] It is possible to provide a magnetic core etc. having stable soft magnetic characteristics using the magnetic core according to the present invention.

[0021] In the magnetic core according to the present invention, the soft magnetic layers may be fragmented so as to have an average crack interval of 0.015 mm or more and 1.0 mm or less.

[0022] In the magnetic core according to the present invention, a space factor of a magnetic material of the magnetic core may be 70.0% or more and 99.5% or less.

[0023] In the magnetic core according to the present invention, $0.020 \leq a \leq 0.100$ may be satisfied.

[0024] In the magnetic core according to the present invention, $0.730 \leq 1 - (a+b+c+d+e+f) \leq 0.950$ may be satisfied.

[0025] In the magnetic core according to the present invention, $\alpha = 0$ may be satisfied.

[0026] In the magnetic core according to the present invention, $\beta = 0$ may be satisfied.

[0027] A coil device according to the present invention includes any of the magnetic cores and a coil.

[0028] A method of manufacturing a magnetic core according to the present invention includes the steps of: fragmenting each of a plurality of soft magnetic ribbons, and laminating the fragmented soft magnetic ribbons in a thickness direction.

BRIEF DESCRIPTION OF THE DRAWINGS

[0029] FIG. 1 is a schematic plane view of a magnetic core according to an embodiment of the present invention.

[0030] FIG. 2 is a schematic cross-sectional view of a magnetic core according to an embodiment of the present invention.

[0031] FIG. 3 is a schematic cross-sectional view of a soft magnetic layer contained in a magnetic core according to an embodiment of the present invention.

[0032] FIG. 4 is a chart obtained by X-ray crystal structure analysis.

[0033] FIG. 5 is a pattern obtained by profile fitting of the chart of FIG. 4.

EMBODIMENTS FOR CARRYING OUT THE INVENTION

[0034] Hereinafter, the present invention is explained based on an embodiment shown in the figures.

[0035] A configuration of a magnetic core **10** according to the present embodiment is explained. FIG. **1** is a schematic plane view viewed from one wide where a center plane A of a cylindrical magnetic core **10** is extended. FIG. **2** is a schematic cross-sectional view of the magnetic core **10** of FIG. **1** cut along the line II-II. FIG. **3** is a schematic cross-sectional view of a soft magnetic layer **12** of FIG. **2** cut along the cutting line III-III. The observation range of FIG. **3** is 4 mm×4 mm.

[0036] As shown in FIG. **2**, the magnetic core **10** according to the present embodiment is formed by alternately laminating a plurality of soft magnetic layers **12** and adhesive layers **14**. FIG. **2** illustrates a case where the magnetic core **10** includes a plurality of soft magnetic layers **12**, but the number of laminated layers may be changed as desired and may be one. When the soft magnetic layers **12** included in the magnetic core according to the present embodiment are plural (e.g., two layers or more and 10000 layers or less), it is most preferable that all of the soft magnetic layers **12** have a plurality of cracks mentioned below.

[0037] The magnetic core **10** of the present embodiment includes the soft magnetic layers **12** and the adhesive layers **14** as main members, but may include other components as long as the effects of the present invention are not impaired. On the contrary, the soft magnetic layers **12** may be laminated without using the adhesive layers **14**.

[0038] Preferably, the volume ratio (space factor) of the magnetic material in the magnetic core **10** is 70% or more and 99.5% or less. When the space factor of the magnetic material is 70% or more, the saturation magnetic flux density can be sufficiently high, and the magnetic core **10** can be effectively used as a magnetic core. When the space factor of the magnetic material is 99.5% or less, the magnetic core **10** is less likely to be damaged and is easy to handle as a magnetic core. The space factor of the magnetic material may be 72% or more and 96% or less. In the present embodiment, the volume of the magnetic material substantially corresponds to that of the soft magnetic layers **12**.

[0039] As shown in FIG. **3**, a plurality of cracks C is formed in each of the soft magnetic layers **12** included in the magnetic core **10** according to the present embodiment. Each of the soft magnetic layers **12** is divided into a plurality of small pieces by the plurality of cracks C. For example, each of the cracks C may have a width of 10 nm or more and 1000 nm or less.

[0040] In the magnetic core **10** according to the present embodiment, a plurality of cracks C is formed in each of the soft magnetic layers **12**, and each of the soft magnetic layers **12** is divided into a plurality of small pieces, so that the change in soft magnetic characteristics due to the stress in the manufacture (particularly, increase in coercivity) is restrained, and a favorable magnetic core **10** can be provided.

[0041] In the present embodiment, when virtual lines B are drawn in a region divided and fragmented by the cracks C, the number of intersections D between the virtual lines B and the cracks C is divided by a total length of the virtual lines B and is defined as an average crack interval.

[0042] Hereinafter, a method of calculating an average crack interval is explained with reference to a specific case

shown in FIG. **3**. FIG. **3** illustrates a square observation area. In FIG. **3**, the cracks C are shown by solid lines, and the virtual lines B are shown by dotted lines.

[0043] The virtual lines B extend in one direction (the horizontal direction in the figure) of the observation area. **10** virtual lines B extend at equal intervals in parallel to the vertical direction of the figure. At this time, the number of intersections D between the virtual lines B and the cracks C is counted. The number of intersections D is a total number of cracks C intersecting the virtual lines B. An average crack interval is obtained by dividing the total length of the virtual lines B by the total number of cracks C intersecting the virtual line B (the number of intersections D) and is represented by Formula (1).

$$\text{Average Crack Interval (mm)} = (\text{Total Length of Virtual Lines B}) / (\text{Number of Intersections D}) \quad \text{Formula (1)}$$

[0044] In the example shown in FIG. **3**, if the observation area is a square (one side: 4 mm), the total length of the virtual lines B is 40 mm, and the number of intersections D is 43, so that the average crack interval is 40/43 [mm] and about 0.93 mm.

[0045] The average crack interval varies depending on a selected observation area and is thereby preferably averaged by being calculated in a plurality of observation areas. Preferably, the average crack interval is averaged by being calculated in three or more different observation areas. Moreover, it is preferable to decide how to select the observation areas. For example, when the ring-shaped magnetic core **10** is used as the present embodiment, the observation areas can be selected to include the center plane A in calculating the average crack interval. Incidentally, the average crack interval is measured in any manner and can be measured, for example, using SEM.

[0046] In the present embodiment, the average crack interval is not limited, but it is preferable that cracks are formed in the soft magnetic layers **12** so that the average crack interval is 0.015 mm or more and 1.0 mm or less. When the average crack interval is smaller than 0.015 mm, the magnetic permeability of the soft magnetic layers **12** is likely to decrease, the inductance Ls of the magnetic core **10** is likely to be low, and the performance of the magnetic core **10** is likely to decrease. When the average crack interval is larger than 1.0 mm, it becomes difficult to punch soft magnetic ribbons with a weak force in a punching step of a method of manufacturing the magnetic core **10** mentioned below. As a result, the stress generated on a cut surface in the punching of soft magnetic ribbons reaches widely, and this reduces the effect of dividing soft magnetic layers into small pieces by a plurality of cracks. Preferably, the average crack interval is 0.015 mm or more and 0.75 mm or less. More preferably, the average crack interval is 0.075 mm or more and 0.75 mm or less.

[0047] Since the magnetic core **10** according to the present embodiment includes the adhesive layers **14**, it is possible to reduce the falling of the small pieces. The adhesive layers **14** can be made of known materials, such as a base body coated with an acrylic type adhesive, an adhesive made of silicone resin, butadiene resin, etc., hot melt, or the like. A PET film is a typical material for the base material. In addition to the PET film, however, the base body may be a resin film, such as a polyimide film, a polyester film, a polyphenylene sulfide (PPS) film, a polypropylene (PP) film, and a fluororesin film like polytetrafluoroethylene (PTFE). Moreover, the adhesive

layers **14** may be an acrylic resin etc. directly applied onto a main surface of the soft magnetic ribbon after a heat treatment mentioned below.

[0048] The magnetic core **10** may include protective films **13** on one end and the other end in the lamination direction (the z-axis direction in FIG. 1 and FIG. 2). The protective films **13** can be known films, such as PET film, polyimide film, and aramid film.

[0049] The soft magnetic layers **12** have a plurality of cracks and are divided into small pieces by the cracks.

[0050] The soft magnetic layers **12** include Fe as a main component,

[0051] the soft magnetic layers have a composition formula of $(\text{Fe}_{(1-(\alpha+\beta))}\text{X1}_{\alpha}\text{X2}_{\beta})_{(1-(a+b+c+d+e+f))}\text{M}_a\text{B}_b\text{P}_c\text{Si}_d\text{C}_e\text{S}_f$ in which X1 is one or more selected from a group consisting of Co and Ni, X2 is one or more selected from a group consisting of Al, Mn, Ag, Zn, Sn, As, Sb, Cu, Cr, Bi, N, O, and rare earth elements, and M is one or more selected from a group consisting of Nb, Hf, Zr, Ta, Mo, V, and W,

[0052] $0 \leq a \leq 0.140$, $0.020 < b \leq 0.200$, $0 \leq c \leq 0.150$, $0 \leq d \leq 0.180$, $0 \leq e < 0.040$, $0 \leq f \leq 0.030$, $\alpha \geq 0$, $\beta \geq 0$, and $0 \leq \alpha + \beta \leq 0.50$ are satisfied, and

[0053] one or more of a, c, and d are larger than zero.

[0054] In addition, a nanohetero structure (the above-mentioned first aspect) or a structure including Fe based nanocrystals (the above-mentioned second aspect) is observed in the soft magnetic layers **12** according to the present embodiment.

[0055] The nanohetero structure refers to a structure including an amorphous phase and fine crystals existing in the amorphous phase. Including an amorphous phase and fine crystals means that the fine crystals are scattered in the amorphous phase. The fact that the fine crystals are scattered in the amorphous phase means that an amorphous ratio X measured by a normal X-ray diffraction (XRD) is 85% or more, and crystal phases can be confirmed by electron diffraction image and high resolution image with transmission electron microscope. The fine crystals refer to crystals each having a particle size of 30 nm or less. Incidentally, the fine crystals may have an average particle size of 0.3-5 nm.

[0056] The Fe based nanocrystals are crystals whose particle size is nano-order (specifically, average particle size: about 30 nm or less) and whose crystal structure of Fe is body-centered cubic (bcc). In the present embodiment, it is preferable to deposit Fe based nanocrystals having an average particle size of 5-30 nm. The structure including Fe based nanocrystals is a structure including Fe based nanocrystals and having an amorphous ratio X of less than 85%.

[0057] When the soft magnetic layers **12** according to the present embodiment has a composition falling within the above-mentioned specific range and a nanohetero structure or a structure including Fe based nanocrystals, the soft magnetic layers **12** easily have cracks by the following fragmentation treatment during the manufacture of the magnetic core **10**. Then, when the soft magnetic layers **12** according to the present embodiment have cracks C, the soft magnetic ribbons **12** can be punched with a weak force. Moreover, it is possible to manufacture the magnetic core **10** whose magnetic characteristics are favorable and whose change in soft magnetic characteristics due to the stress during manufacture (particularly, increase in coercivity) is restrained.

[0058] Moreover, when the soft magnetic layers have a structure including Fe based nanocrystals, the saturation magnetic flux density is likely to be high, and the coercivity is likely to be low.

[0059] Hereinafter, the composition of the soft magnetic layers **12** according to the present embodiment is explained in more detail.

[0060] M is one or more selected from a group consisting of Nb, Hf, Zr, Ta, Ti, Mo, V, and W. Preferably, M is Nb.

[0061] The M content (a) satisfies $0 \leq a \leq 0.140$. That is, M may not be contained. When M is not contained, however, the magnetostriction constant tends to be high, and the coercivity tends to be high. The M content (a) is preferably $0.020 \leq a \leq 0.100$, more preferably $0.040 \leq a \leq 0.100$, and still more preferably $0.050 \leq a \leq 0.080$. When the M content (a) is large, the coercivity easily increases in the manufacture of the magnetic core **10**.

[0062] The B content (b) satisfies $0.020 < b \leq 0.200$. The B content (b) is preferably $0.025 \leq b \leq 0.200$, more preferably $0.025 \leq b \leq 0.120$, and most preferably $0.060 \leq b \leq 0.120$. When the B content (b) is small, a crystal phase composed of crystals having a particle size of larger than 30 nm is easily generated in the manufacture of soft magnetic alloy ribbons mentioned below, and it is difficult to obtain the nanohetero structure or the structure including Fe based nanocrystals. When the B content (b) is large, the coercivity easily increases in the manufacture of the magnetic core **10**.

[0063] The P content (c) satisfies $0 \leq c \leq 0.150$. That is, P may not be contained. When P is contained, the coercivity easily decreases. From the viewpoint of reducing the coercivity and improving the inductance Ls of the magnetic core **10**, $0.050 \leq c \leq 0.150$ is preferable, and $0.050 \leq c \leq 0.080$ is more preferable. From the viewpoint of making it difficult to increase the coercivity in the manufacture of the magnetic core **10**, $0 \leq c \leq 0.030$ is preferable. When the P content (c) is large, the coercivity easily increases in the manufacture of the magnetic core **10**.

[0064] The Si content (d) satisfies $0 \leq d \leq 0.180$. That is, Si may not be contained. $0 \leq d \leq 0.175$ may be satisfied. Preferably, $0 \leq d \leq 0.060$ is satisfied. When $0.070 \leq d \leq 0.180$ is satisfied, the soft magnetic layers **12** and the magnetic core **10** having favorable soft magnetic characteristics tend to be easily obtained by reducing the M content (a) and the P content (c).

[0065] The C content (e) satisfies $0 \leq e < 0.040$. That is, C may not be contained. From the viewpoint of reducing the coercivity, $0 \leq e \leq 0.030$ is preferable, and $0.001 \leq e \leq 0.010$ is more preferable. When the C content (e) is large, the coercivity easily increases in the manufacture of the magnetic core **10**.

[0066] The S content (f) satisfies $0 \leq f \leq 0.030$. That is, S may not be contained. From the viewpoint of reducing coercivity, $0 \leq f \leq 0.001$ is preferable. When the S content (f) is large, a crystal phase composed of crystals having a particle size of larger than 30 nm is easily generated in the manufacture of soft magnetic alloy ribbons mentioned below, and it is difficult to obtain the nanohetero structure or the structure including Fe based nanocrystals.

[0067] One or more of "a", "c", and "d" are larger than zero. One or more of "a", "c", and "d" may be 0.001 or more or may be 0.010 or more. That is, the soft magnetic layers **12** according to the present embodiment contains one or

more of M, P, and Si. This makes it easy to obtain the nanohetero structure or the structure including Fe based nanocrystals.

[0068] The Fe content $\{(1-(a+b+c+d+e+f))\}$ is not limited, but $0.730 \leq 1-(a+b+c+d+e+f) \leq 0.950$ is preferably satisfied. More preferably, $0.730 \leq 1-(a+b+c+d+e+f) \leq 0.900$ is preferably satisfied. When $0.730 < 1-(a+b+c+d+e+f)$ is satisfied, saturation magnetic flux density is easily improved. When $1-(a+b+c+d+e+f) \leq 0.950$ is satisfied, it is easy to obtain the nanohetero structure or the structure including Fe based nanocrystals.

[0069] In the soft magnetic alloy according to the present embodiment, a part of Fe may be substituted by X1 and/or X2.

[0070] X1 is one or more selected from a group consisting of Co and Ni. The X1 content (α) may be $\alpha=0$. That is, X1 may not be contained. Preferably, the number of atoms of X1 is 40 at % or less if the number of atoms of the entire composition is 100 at %. That is, $0 \leq \alpha \{1-(a+b+c+d+e+f)\} \leq 0.40$ is preferably satisfied.

[0071] X2 is one or more selected from a group consisting of Al, Mn, Ag, Zn, Sn, As, Sb, Cu, Cr, Bi, N, O, and rare earth elements. The content X2 (β) may be $\beta=0$. That is, X2 may not be contained. Preferably, the number of atoms of X2 is 3.0 at % or less if the number of atoms of the entire composition is 100 at %. That is, $0 \leq \beta \{1-(a+b+c+d+e+f)\} \leq 0.030$ is preferably satisfied.

[0072] The substitution amount of Fe by X1 and/or X2 is half or less of Fe based on the number of atoms. That is, $0 \leq \alpha + \beta \leq 0.50$ is satisfied. When $\alpha + \beta > 0.50$ is satisfied, it is difficult to obtain the nanohetero structure or the structure including Fe based nanocrystals.

[0073] Incidentally, the soft magnetic layers 12 according to the present embodiment may contain elements other than the above-mentioned elements as unavoidable impurities as long as the characteristics are not affected. For example, 1 wt % or less of unavoidable impurities may be contained with respect to 100 wt % of the soft magnetic layers 12.

[0074] Hereinafter, explained is a method of manufacturing the magnetic core 10 according to the present embodiment.

[0075] First, explained is a method of manufacturing a soft magnetic ribbon to be the soft magnetic layers 12 included in the magnetic core 10 by lamination. Hereinafter, the soft magnetic ribbon may be simply referred to as a ribbon.

[0076] The soft magnetic ribbons are manufactured in any manner. For example, the soft magnetic ribbons according to the present embodiment are manufactured by a single-roller melt-spinning method. The ribbons may be continuous ribbons.

[0077] In the single-roller melt-spinning method, pure metals of respective metal elements contained in a soft magnetic alloy finally obtained are initially prepared and weighed so that a composition identical to that of the soft magnetic alloy finally obtained is obtained. Then, the pure metals of the respective metal elements are melted and mixed to make a base alloy. Incidentally, the pure metals are melted in any manner. For example, the pure metals are melted by high-frequency heating after a chamber is evacuated. Incidentally, the base alloy and the soft magnetic alloy including Fe based nanocrystals finally obtained normally have the same composition.

[0078] Next, the prepared base alloy is melted by heating to obtain a molten metal. The temperature of the molten metal is not limited and may be, for example, 1100-1350° C.

[0079] In the single-roller melt-spinning method, the thickness of the ribbon to be obtained can be controlled by mainly controlling the rotating speed of the roller, but can also be controlled by, for example, controlling the distance between the nozzle and the roller, the temperature of the molten metal, or the like. The thickness of the ribbon is not limited, but may be 14-30 for example. Incidentally, the thickness of the ribbon and the thickness of each of the soft magnetic layers 12 included in the magnetic core 10 to be finally obtained are substantially the same.

[0080] There is no limit to the temperature and the rotation speed of the roller or the atmosphere inside the chamber. The temperature of the roller is substantially a room temperature or higher and 80° C. or lower. The lower the temperature of the roller is, the smaller the average grain size of the fine crystals tends to be. The higher the rotation speed of the roller is, the smaller the average grain size of the fine crystals tends to be. For example, the rotation speed of the roller is 10-30 m/sec. From the viewpoint of cost, the atmosphere inside the chamber is preferably atmospheric air.

[0081] Before a heat treatment mentioned below, the ribbon has an amorphous structure, that is, a structure composed of only amorphous phases or the nanohetero structure. A ribbon having a structure including Fe based nanocrystals can be obtained by being subjected to a heat treatment mentioned below. A ribbon having the nanohetero structure may be obtained by the heat treatment.

[0082] Whether the ribbon of the soft magnetic alloy has an amorphous structure or a crystal structure can be confirmed by a normal X-ray diffraction measurement (XRD).

[0083] Specifically, an X-ray structural analysis is carried out by XRD to calculate an amorphous ratio X (%) shown by the following formula (1). When the amorphous ratio X (%) is 85% or more, the ribbon of the soft magnetic alloy has an amorphous structure. When the amorphous ratio X (%) is less than 85%, the ribbon of the soft magnetic alloy has a crystal structure.

$$X (\%) = 100 - (I_c / (I_c + I_a) \times 100) \quad (1)$$

[0084] I_c : scattering integrated intensity of crystal phase

[0085] I_a : scattering integrated intensity of amorphous phase

[0086] For calculation of the amorphous ratio X, the soft magnetic alloy according to the present embodiment is subjected to an X-ray crystal structural analysis by XRD to obtain the chart shown in FIG. 4. This chart is subjected to a profile fitting using the Lorentz function of the following formula (2).

$$f(x) = \frac{h}{1 + \frac{(x-u)^2}{w^2}} + b \quad (2)$$

[0087] h : peak height

[0088] u : peak position

[0089] w : half-value width

[0090] b : background height

[0091] As a result of the profile fitting, obtained are a crystalline component pattern α_c denoting a scattering integrated intensity of crystal phase, an amorphous component

pattern α_a denoting a scattering integrated intensity of amorphous phase, and a pattern α_{c+a} obtained by combining them shown in FIG. 5. From the obtained patterns, obtained are a scattering integrated intensity of crystal phase Ic and a scattering integrated intensity of amorphous phase Ia. Incidentally, the measurement range is a diffraction angle 2θ , in which a halo derived from amorphousness can be confirmed, and is specifically $2\theta=30^\circ$ to 60° . In this range, an error between the actually measured integrated intensity with XRD and the integrated intensity calculated by the Lorentz function is set to be within 1%.

[0092] In the present embodiment, when the soft magnetic alloy is obtained in the shape of a ribbon by the single-roller melt-spinning method mentioned below, an amorphous ratio (X_A) on the surface in contact with the roller surface and an amorphous ratio (X_B) on the surface not in contact with the roller surface may be different from each other. In this case, an average of the X_A and the X_B is an amorphous ratio X .

[0093] The ribbon before the heat treatment may have a structure composed of only amorphous phases, but preferably has a nanohetero structure. The grain size of the fine crystals in the nanohetero structure is not limited, but the average grain size is preferably 0.3-5 nm.

[0094] The existence and average particle size of the fine crystals in case of a nanohetero structure can be observed by, for example, obtaining an electron diffraction image and a high resolution image of a sample thinned by ion milling using a transmission electron microscope. When an electron diffraction image is used, a ring-shaped diffraction is formed in case of a structure composed of only amorphous phases in the diffraction pattern, whereas diffraction spots caused by the fine crystals are generated in case of a structure including fine crystals. When a high resolution image is used, the existence and average particle size of the fine crystals can be observed visually at a magnification of 1.00×10^5 to 3.00×10^5 .

[0095] There is no limit to heat treatment conditions for manufacturing a ribbon having a structure including Fe based nanocrystals or a ribbon having a nanohetero structure. The preferable heat treatment conditions differ depending on the composition of the soft magnetic ribbon. Normally, a heat-treatment temperature is preferably about $400-700^\circ\text{C}$., and a heat-treatment time is preferably about 0.1-6 hours, but favorable heat-treatment temperature and heat-treatment time may be in a range deviated from the above ranges depending on the composition. The heat treatment is carried out in any atmosphere, such as an active atmosphere of air and an inert atmosphere of Ar gas, N_2 gas, etc. Due to the heat treatment, the soft magnetic ribbon becomes brittle and is turned into a state easily subjected to a fragmentation treatment. In addition, residual strain in the soft magnetic ribbon is removed.

[0096] Incidentally, if the ribbon has a nanohetero structure at the stage of being manufactured, no heat treatment may be carried out. For the above-mentioned reasons, however, the heat treatment is preferably carried out. The heat treatment may be carried out after the manufacture of the magnetic core 10 mentioned below.

[0097] The average grain size of crystals contained in the obtained soft magnetic ribbon is calculated in any manner, such as observation using a transmission electron microscope. The crystal structure of body-centered cubic (bcc) structure is also confirmed in any manner, such as X-ray diffraction measurement.

[0098] A method of manufacturing a magnetic core 10 according to the present embodiment mainly includes an adhesive-layer formation step, a crack formation step (fragmentation step), a punching step, and a lamination step. Hereinafter, the outline of each step is explained.

(Adhesive-Layer Formation Step)

[0099] The adhesive layer is formed on each of the soft magnetic ribbons subjected to the heat treatment. The adhesive layer can be formed using a known method. For example, the adhesive layer may be formed by thinly applying a solution containing a resin to the soft magnetic ribbons and drying the solvent. In addition, a double-sided tape may be adhered to the soft magnetic ribbons as an adhesive layer. For example, the double-sided tape is a polyethylene terephthalate (PET) film whose both surfaces are coated with an adhesive.

(Crack Formation Step (Fragmentation Step))

[0100] Each of the multiple soft magnetic ribbons with the adhesive layers is fragmented by generating cracks. A known method can be used for the generation of cracks. For example, cracks may be generated by applying an external force to the soft magnetic ribbons. For example, applying an external force to the soft magnetic ribbons is carried out by pressing with a mold, bending through a rolling roller, or the like. The mold and the rolling roller may be provided with a predetermined uneven pattern.

[0101] Then, each of the soft magnetic ribbons is fragmented by generating a plurality of cracks so that the average crack interval is within the above-mentioned range. The average crack interval is controlled in any manner. When the soft magnetic ribbons are pressed to be fragmented with a mold, for example, the average crack interval can be appropriately changed by changing the pressure during pressing. When the soft magnetic ribbons are bent through a rolling roller, for example, the average crack interval can be appropriately changed by changing the number of times where the soft magnetic ribbons are passed through the rolling roller.

[0102] When the adhesive layers are formed in advance, it becomes easy to prevent small pieces divided by the cracks from scattering. That is, the soft magnetic ribbons after forming the cracks are divided into a plurality of small pieces, but the locations of all of the small pieces are fixed via the adhesive layers, and the shape before forming the cracks is thereby substantially maintained as a whole. If the cracks can be formed while maintaining the overall shape of the soft magnetic ribbons even without using the adhesive layers, however, the adhesive layers are not necessarily formed before the cracks are formed.

(Punching Step)

[0103] Next, each of the multiple fragmented soft magnetic ribbons with the cracks is punched into a predetermined shape. In the present embodiment, as shown in FIG. 1, a central part of each of the ribbons is punched into a circular shape. The punching step can be carried out using a known method. For example, the punching step can be performed by sandwiching the soft magnetic ribbons between a punching die having a desired shape and a facing plate and pressurizing them from the facing plate to the punching die or from the punching die to the facing plate.

Incidentally, when the adhesive layers are formed on the soft magnetic ribbons before the punching, the soft magnetic ribbons are punched together with the adhesive layers.

[0104] The soft magnetic ribbons composed of the soft magnetic material according to the present embodiment is hard and is thereby difficult to be punched with a weak force. When the soft magnetic ribbons are punched, a stress is generated by cutting the punched portion and the remaining portion. The stronger the force of the punching is, the larger the stress becomes. This stress is transmitted to the remaining portion of the soft magnetic ribbons and deteriorates soft magnetic characteristics. That is, coercivity becomes large.

[0105] However, each of the soft magnetic ribbons according to the present embodiment has cracks and is fragmented. Thus, each of the soft magnetic ribbons according to the present embodiment can be punched with a weaker force compared to when a soft magnetic ribbon has no cracks and is not fragmented. Thus, the stress becomes small. Moreover, the portion near the cut surface where the stress is generated at the time of punching and the other portion are physically distant from each other. Thus, the stress is not transmitted to most part other than the portion near the cut surface. Then, the deterioration of soft magnetic characteristics caused by the stress can be minimized.

[0106] Therefore, in the soft magnetic ribbons according to the present embodiment, the deterioration of soft magnetic characteristics due to punching (increase in coercivity) is reduced, and the soft magnetic characteristics of the magnetic core **10** finally obtained are improved. Furthermore, since the soft magnetic ribbons according to the present embodiment can be punched with a comparatively weak force, the soft magnetic ribbons can be easily processed into a desired shape and is excellent in productivity.

(Lamination Step)

[0107] The magnetic core **10** according to the present embodiment can be obtained by overlapping and laminating the multiple punched soft magnetic ribbons via the adhesive layers in the thickness direction. Protective films **13** may be formed on one end and the other end in the lamination direction (the z-axis direction in FIG. **1** and FIG. **2**). The protective films **13** are formed in any manner.

[0108] Incidentally, the steps other than the crack formation step and the lamination step are not essential steps. Furthermore, the order of each step may be rearranged appropriately.

[0109] The magnetic core **10** according to the present embodiment has a structure in which the space factor of the magnetic material (the soft magnetic layers **12**) is increased by laminating a plurality of soft magnetic ribbons and is strong and easy to handle.

[0110] Since the magnetic core **10** according to the present embodiment is formed by laminating a plurality of soft magnetic ribbons, the current path is divided at a plurality of locations in the lamination direction. In the magnetic core **10** according to the present embodiment, since each of the soft magnetic ribbons (the soft magnetic layers **12**) has cracks and is fragmented, the current path is also divided at a plurality of locations in a direction intersecting the lamination direction. Therefore, in the coil device according to the present embodiment, the eddy current path accompanying the change of the magnetic flux in the alternating magnetic field is divided in all directions, and the eddy current loss can be greatly reduced.

[0111] FIG. **1** illustrates a cylindrical magnetic core, but the magnetic core according to the present embodiment may have any known shape, such as a rectangular cylindrical shape. The magnetic core according to the present embodiment may be formed by combining a plurality of cores, such as E-type cores.

[0112] The magnetic core **10** is used for any purposes, such as for coil devices including a conductor (e.g., transformer, choke coil, magnetic sensor).

EXAMPLES

Experimental Example 1

<Preparation of Soft Magnetic Ribbon>

[0113] Raw material metals were weighed so as to have the alloy composition of each example and comparative example shown in the following tables and were melted by high frequency heating to prepare base alloys.

[0114] After that, the prepared base alloys were melted by heating and turned into a molten metal at 1250° C. This metal was sprayed against a roller of 60° C. rotating at 20 m/sec. in the air (single-roller melt-spinning method) to form a ribbon. Incidentally, the thickness of the ribbon was about 20 μ m and the width of the ribbon was about 50 mm.

[0115] Next, whether the obtained ribbon had an amorphous structure (a structure composed of only amorphous phases or a nanohetero structure) or a crystal structure was determined by a normal X-ray diffraction (XRD) measurement. The results are shown in Table 1.

[0116] After that, a heat treatment was carried out for the ribbons of all examples except for Samples 1 and 12 in Tables 1 and 2. The heat treatment conditions of Samples 2-6 and 13-17 were 500° C. (heat treatment temperature), 60 minutes (holding time), 1° C./min (heating rate), and 1° C./min (cooling rate). The heat treatment conditions of Samples 7-11 and 18-22 were 570° C. (heat treatment temperature), 60 minutes (holding time), 1° C./min (heating rate), and 1° C./min (cooling rate).

<Evaluation of Soft Magnetic Ribbons>

[0117] The fine structure of each ribbon after the heat treatment was confirmed by X-ray diffraction measurement (XRD) and observation using a transmission electron microscope (TEM). Specifically, observed was which structure (a structure including Fe based nanocrystals, a nanohetero structure, or a structure composed of only amorphous phases) each of the ribbons had. Incidentally, the structure including Fe based nanocrystals was bcc.

[0118] Then, when the fine structure of each ribbon after the heat treatment was a nanohetero structure, it was confirmed that the average grain size of the fine crystals was 0.3-5.0 nm in all Examples. When the fine structure of each ribbon after the heat treatment was a structure including Fe based nanocrystals, it was confirmed that the average grain size of the Fe based nanocrystals was 5.0 nm or more and 30 nm or less in all examples.

[0119] Furthermore, a saturation magnetic flux density B_s and a coercivity H_{ca} of each ribbon after the heat treatment were measured. The saturation magnetic flux density was measured in a magnetic field of 1000 kA/m using a vibrating sample magnetometer (VSM). The coercivity was measured in a magnetic field of 5 kA/m using a DC BH tracer.

<Manufacture of Magnetic Core>

[0120] First, a resin solution was applied to the obtained soft magnetic ribbons. Then, the solvent was dried, and adhesive layers each having a thickness of about 1-2 μm were formed on both surfaces of each of the soft magnetic ribbons to manufacture a magnetic sheet having the adhesive layers.

[0121] Next, the manufactured magnetic sheet was subjected to a crack formation treatment so that the average crack interval of each of the soft magnetic ribbons would be the value shown in Table 2, and a fragmented magnetic sheet was manufactured. Incidentally, the magnetic sheets of Samples 1 and 12, which used the soft magnetic ribbons whose fine structure was amorphous, could not form cracks and could not be fragmented.

[0122] Next, the fragmented magnetic sheet was punched into a ring shape (outer diameter: 18 mm, inner diameter: 10 mm). Specifically, this punching was performed by sandwiching the fragmented magnetic sheet between a punching die and a facing plate and applying pressure from the facing plate to the punching die. Incidentally, the magnetic sheets of Samples 1 and 12, which could not be fragmented, could not be punched with a force equivalent to that of the fragmented magnetic sheets of the other examples.

[0123] Next, the punched-out fragmented magnetic sheets were attached to each other so as to have a height of about 5 mm and laminated to obtain a magnetic core. The space factor of the obtained soft magnetic layers of the magnetic core was about 85%. Furthermore, 30 magnetic cores were manufactured for each sample in the same procedure.

<Evaluation of Magnetic Cores>

[0124] As with the coercivity H_{ca} of the ribbons, the coercivity H_{cb} of the magnetic cores was measured in a magnetic field of 5 kA/m using a DC BH tracer. The coercivity of each of the 30 magnetic cores was measured and averaged to obtain H_{cb} .

[0125] Then, a change in coercivity $\Delta H_c (=H_{cb}-H_{ca})$ was calculated from the obtained H_{ca} and H_{cb} . In addition, a coercivity change rate (%) was calculated. Specifically, the coercivity change rate (%) was calculated by substituting ΔH_c and H_{ca} into the formula of $(\Delta H_c/H_{ca}) \times 100(\%)$. A coercivity change rate of less than 100% was regarded as favorable.

[0126] Finally, a coil was wound around each of the magnetic cores along the circumferential direction to form 30 coil devices, and the inductance of each coil at 100 kHz was measured using an LCR meter and averaged to obtain L_s .

TABLE 1

| Sample No. | Example/ Comparative Example | Composition | XRD Before Heat Treatment | Heat Treatment | Fine Structure After Heat Treatment | Saturation Magnetic Flux Density of Ribbons B_s (T) | Coercivity of Ribbons H_{ca} (A/m) |
|------------|---------------------------------|---|---------------------------|----------------|-------------------------------------|---|--------------------------------------|
| 1 | Comp. Ex. | Fe _{0.735} Nb _{0.03} B _{0.09} Si _{0.135} Cu _{0.01} | amorphous | no | amorphous | 1.17 | 2.10 |
| 2 | Ex. | Fe _{0.735} Nb _{0.03} B _{0.09} Si _{0.135} Cu _{0.01} | amorphous | yes | nanothero | 1.18 | 1.20 |
| 3 | Ex. | Fe _{0.735} Nb _{0.03} B _{0.09} Si _{0.135} Cu _{0.01} | amorphous | yes | nanothero | 1.18 | 1.20 |
| 4 | Ex. | Fe _{0.735} Nb _{0.03} B _{0.09} Si _{0.135} Cu _{0.01} | amorphous | yes | nanothero | 1.18 | 1.20 |
| 4a | Ex. | Fe _{0.735} Nb _{0.03} B _{0.09} Si _{0.135} Cu _{0.01} | amorphous | yes | nanothero | 1.18 | 1.20 |
| 4b | Ex. | Fe _{0.735} Nb _{0.03} B _{0.09} Si _{0.135} Cu _{0.01} | amorphous | yes | nanothero | 1.18 | 1.20 |
| 5 | Ex. | Fe _{0.735} Nb _{0.03} B _{0.09} Si _{0.135} Cu _{0.01} | amorphous | yes | nanothero | 1.18 | 1.20 |
| 5a | Ex. | Fe _{0.735} Nb _{0.03} B _{0.09} Si _{0.135} Cu _{0.01} | amorphous | yes | nanothero | 1.18 | 1.20 |
| 5b | Ex. | Fe _{0.735} Nb _{0.03} B _{0.09} Si _{0.135} Cu _{0.01} | amorphous | yes | nanothero | 1.18 | 1.20 |
| 6 | Ex. | Fe _{0.735} Nb _{0.03} B _{0.09} Si _{0.135} Cu _{0.01} | amorphous | yes | nanothero | 1.18 | 1.20 |
| 7 | Ex. | Fe _{0.735} Nb _{0.03} B _{0.09} Si _{0.135} Cu _{0.01} | amorphous | yes | Fe based nanocrystal | 1.21 | 0.50 |
| 8 | Ex. | Fe _{0.735} Nb _{0.03} B _{0.09} Si _{0.135} Cu _{0.01} | amorphous | yes | Fe based nanocrystal | 1.21 | 0.50 |
| 9 | Ex. | Fe _{0.735} Nb _{0.03} B _{0.09} Si _{0.135} Cu _{0.01} | amorphous | yes | Fe based nanocrystal | 1.21 | 0.50 |
| 9a | Ex. | Fe _{0.735} Nb _{0.03} B _{0.09} Si _{0.135} Cu _{0.01} | amorphous | yes | Fe based nanocrystal | 1.21 | 0.50 |
| 9b | Ex. | Fe _{0.735} Nb _{0.03} B _{0.09} Si _{0.135} Cu _{0.01} | amorphous | yes | Fe based nanocrystal | 1.21 | 0.50 |
| 10 | Ex. | Fe _{0.735} Nb _{0.03} B _{0.09} Si _{0.135} Cu _{0.01} | amorphous | yes | Fe based nanocrystal | 1.21 | 0.50 |
| 10a | Ex. | Fe _{0.735} Nb _{0.03} B _{0.09} Si _{0.135} Cu _{0.01} | amorphous | yes | Fe based nanocrystal | 1.21 | 0.50 |
| 10b | Ex. | Fe _{0.735} Nb _{0.03} B _{0.09} Si _{0.135} Cu _{0.01} | amorphous | yes | Fe based nanocrystal | 1.21 | 0.50 |
| 11 | Ex. | Fe _{0.735} Nb _{0.03} B _{0.09} Si _{0.135} Cu _{0.01} | amorphous | yes | Fe based nanocrystal | 1.21 | 0.50 |
| 12 | Comp. Ex. | Fe _{0.84} Nb _{0.07} B _{0.09} | amorphous | no | amorphous | 0.50 | 2.10 |
| 13 | Ex. | Fe _{0.84} Nb _{0.07} B _{0.09} | amorphous | yes | nanothero | 1.34 | 4.80 |
| 14 | Ex. | Fe _{0.84} Nb _{0.07} B _{0.09} | amorphous | yes | nanothero | 1.34 | 4.80 |
| 15 | Ex. | Fe _{0.84} Nb _{0.07} B _{0.09} | amorphous | yes | nanothero | 1.34 | 4.80 |
| 15a | Ex. | Fe _{0.84} Nb _{0.07} B _{0.09} | amorphous | yes | nanothero | 1.34 | 4.80 |
| 15b | Ex. | Fe _{0.84} Nb _{0.07} B _{0.09} | amorphous | yes | nanothero | 1.34 | 4.80 |
| 16 | Ex. | Fe _{0.84} Nb _{0.07} B _{0.09} | amorphous | yes | nanothero | 1.34 | 4.80 |
| 16a | Ex. | Fe _{0.84} Nb _{0.07} B _{0.09} | amorphous | yes | nanothero | 1.34 | 4.80 |
| 16b | Ex. | Fe _{0.84} Nb _{0.07} B _{0.09} | amorphous | yes | nanothero | 1.34 | 4.80 |
| 17 | Ex. | Fe _{0.84} Nb _{0.07} B _{0.09} | amorphous | yes | nanothero | 1.34 | 4.80 |
| 18 | Ex. | Fe _{0.84} Nb _{0.07} B _{0.09} | amorphous | yes | Fe based nanocrystal | 1.51 | 5.50 |
| 19 | Ex. | Fe _{0.84} Nb _{0.07} B _{0.09} | amorphous | yes | Fe based nanocrystal | 1.51 | 5.50 |
| 20 | Ex. | Fe _{0.84} Nb _{0.07} B _{0.09} | amorphous | yes | Fe based nanocrystal | 1.51 | 5.50 |
| 20a | Ex. | Fe _{0.84} Nb _{0.07} B _{0.09} | amorphous | yes | Fe based nanocrystal | 1.51 | 5.50 |
| 20b | Ex. | Fe _{0.84} Nb _{0.07} B _{0.09} | amorphous | yes | Fe based nanocrystal | 1.51 | 5.50 |
| 21 | Ex. | Fe _{0.84} Nb _{0.07} B _{0.09} | amorphous | yes | Fe based nanocrystal | 1.51 | 5.50 |
| 21a | Ex. | Fe _{0.84} Nb _{0.07} B _{0.09} | amorphous | yes | Fe based nanocrystal | 1.51 | 5.50 |
| 21b | Ex. | Fe _{0.84} Nb _{0.07} B _{0.09} | amorphous | yes | Fe based nanocrystal | 1.51 | 5.50 |
| 22 | Ex. | Fe _{0.84} Nb _{0.07} B _{0.09} | amorphous | yes | Fe based nanocrystal | 1.51 | 5.50 |

TABLE 2

| Sample No. | Example/Comparative Example | Fragmentation | Average Crack Interval (mm) | Punching Possibility | Coercivity of Core H _{cb} (A/m) | ΔH_c [H _{cb} - H _{ca}] (A/m) | Coercivity Change Rate (%) | L _s (μ H) |
|------------|-----------------------------|---------------|-----------------------------|----------------------|--|---|----------------------------|---------------------------|
| 1 | Comp. Ex. | impossible | — | impossible | — | — | — | — |
| 2 | Ex. | yes | 0.17 | possible | 2.21 | 1.01 | 84 | 346 |
| 3 | Ex. | yes | 0.50 | possible | 2.12 | 0.92 | 77 | 552 |
| 4 | Ex. | yes | 0.015 | possible | 2.21 | 1.01 | 84 | 33 |
| 4a | Ex. | yes | 0.030 | possible | 2.22 | 1.02 | 85 | 76 |
| 4b | Ex. | yes | 0.075 | possible | 2.22 | 1.02 | 85 | 190 |
| 5 | Ex. | yes | 0.010 | possible | 2.28 | 1.08 | 90 | 20 |
| 5a | Ex. | yes | 0.10 | possible | 2.21 | 1.01 | 84 | 250 |
| 5b | Ex. | yes | 0.30 | possible | 2.19 | 0.99 | 83 | 480 |
| 6 | Ex. | yes | 0.75 | possible | 2.21 | 1.01 | 84 | 626 |
| 7 | Ex. | yes | 0.17 | possible | 0.86 | 0.36 | 72 | 356 |
| 8 | Ex. | yes | 0.50 | possible | 0.82 | 0.32 | 65 | 598 |
| 9 | Ex. | yes | 0.015 | possible | 0.86 | 0.36 | 73 | 33 |
| 9a | Ex. | yes | 0.030 | possible | 0.88 | 0.38 | 76 | 83 |
| 9b | Ex. | yes | 0.075 | possible | 0.85 | 0.35 | 70 | 210 |
| 10 | Ex. | yes | 0.010 | possible | 0.90 | 0.40 | 80 | 20 |
| 10a | Ex. | yes | 0.10 | possible | 0.88 | 0.38 | 76 | 254 |
| 10b | Ex. | yes | 0.30 | possible | 0.83 | 0.33 | 66 | 504 |
| 11 | Ex. | yes | 0.75 | possible | 0.79 | 0.29 | 59 | 701 |
| 12 | Comp. Ex. | impossible | — | impossible | — | — | — | — |
| 13 | Ex. | yes | 0.17 | possible | 8.64 | 3.84 | 80 | 322 |
| 14 | Ex. | yes | 0.50 | possible | 8.27 | 3.47 | 72 | 472 |
| 15 | Ex. | yes | 0.015 | possible | 8.75 | 3.95 | 82 | 33 |
| 15a | Ex. | yes | 0.030 | possible | 8.70 | 3.90 | 81 | 75 |
| 15b | Ex. | yes | 0.075 | possible | 8.55 | 3.75 | 78 | 188 |
| 16 | Ex. | yes | 0.010 | possible | 8.57 | 3.77 | 79 | 20 |
| 16a | Ex. | yes | 0.10 | possible | 8.55 | 3.75 | 78 | 240 |
| 16b | Ex. | yes | 0.30 | possible | 8.50 | 3.70 | 77 | 418 |
| 17 | Ex. | yes | 0.75 | possible | 8.34 | 3.54 | 74 | 514 |
| 18 | Ex. | yes | 0.17 | possible | 9.36 | 3.86 | 70 | 346 |
| 19 | Ex. | yes | 0.50 | possible | 9.14 | 3.64 | 66 | 554 |
| 20 | Ex. | yes | 0.015 | possible | 9.33 | 3.83 | 70 | 33 |
| 20a | Ex. | yes | 0.030 | possible | 9.31 | 3.81 | 69 | 80 |
| 20b | Ex. | yes | 0.075 | possible | 9.30 | 3.80 | 69 | 190 |
| 21 | Ex. | yes | 0.010 | possible | 9.32 | 3.82 | 70 | 20 |
| 21a | Ex. | yes | 0.10 | possible | 9.33 | 3.83 | 70 | 257 |
| 21b | Ex. | yes | 0.30 | possible | 9.24 | 3.74 | 68 | 483 |
| 22 | Ex. | yes | 0.75 | possible | 9.09 | 3.59 | 65 | 637 |

[0127] According to Table 1 and Table 2, the soft magnetic ribbon of each example was able to be fragmented and punched, and the magnetic cores of each example had a favorable coercivity change rate. The reason why the magnetic cores of each example had a favorable coercivity change rate is explained below.

[0128] Since the soft magnetic ribbons were fragmented, the force during punching was able to be reduced. In addition, since the soft magnetic ribbons were fragmented, the stress generated near the cross section at the time of punching was less likely to be transmitted to the inside. As a result, the deterioration of soft magnetic characteristics (increase in coercivity and decrease in inductance) was restrained. In addition, the inductance L_s was higher as the average crack interval was larger and the size of each small piece was larger.

[0129] On the other hand, the soft magnetic ribbons of each comparative example, whose fine structure was amorphous, could not be fragmented or punched.

[0130] When the fine structure was a nanohetero structure or a structure including Fe based nanocrystals, the soft magnetic ribbons were able to be fragmented probably because the crystal grain boundaries served as a starting point of fragmentation at the time of applying an external force. On the other hand, the reason why the soft magnetic ribbons could not be fragmented when the fine structure was amorphous was that there were no grain boundaries or starting points of fragmentation.

Experimental Example 2

[0131] Except for changing the composition of the soft magnetic ribbons within the ranges shown in Tables 3-12, Experimental Example 2 was carried out with the same conditions as Samples No. 7-11 of Experimental Example 1.

TABLE 3

| | | | | | | | | | | Saturation Magnetic Flux | Coer- civity of | Average | Coer- civity of | ΔH_c | Coer- civity | | |
|-----------------------------------|-----------|---|--------|--------|---------|--------|--------|----------------------------------|---------------------------------|--------------------------------|---------------------------|----------------------|-------------------------|-----------------------|-------------------|-----|--|
| Example/ Sample No. Example | | $Fe(1 - (a + b + c + d + e + f))MaBbPcSidCeSf_XRD$ | | | | | | | Density of Ribbons Bs (T) | Ribbons Hca (A/m) | Crack Interval (mm) | Core Hcb (A/m) | [Hcb - Hca] (A/m) | Change Rate (%) | Ls (μH) | | |
| | | M (Nb) Fe | B a | P b | Si c | C d | S e | Before Heat Treatment f | | | | | | | | | |
| 24 | Ex. | 0.840 | 0.020 | 0.090 | 0.050 | 0.000 | 0.000 | 0.000 | amorphous | 1.58 | 2.80 | 0.17 | 4.84 | 2.04 | 73 | 351 | |
| 25 | Ex. | 0.820 | 0.040 | 0.090 | 0.050 | 0.000 | 0.000 | 0.000 | amorphous | 1.56 | 2.40 | 0.17 | 4.23 | 1.83 | 76 | 359 | |
| 26 | Ex. | 0.810 | 0.050 | 0.090 | 0.050 | 0.000 | 0.000 | 0.000 | amorphous | 1.53 | 1.90 | 0.17 | 3.35 | 1.45 | 76 | 371 | |
| 45 | Ex. | 0.800 | 0.060 | 0.090 | 0.050 | 0.000 | 0.000 | 0.000 | amorphous | 1.50 | 1.80 | 0.17 | 3.33 | 1.53 | 85 | 370 | |
| 27 | Ex. | 0.780 | 0.080 | 0.090 | 0.050 | 0.000 | 0.000 | 0.000 | amorphous | 1.48 | 1.80 | 0.17 | 3.39 | 1.59 | 88 | 369 | |
| 28 | Ex. | 0.760 | 0.100 | 0.090 | 0.050 | 0.000 | 0.000 | 0.000 | amorphous | 1.44 | 2.30 | 0.17 | 4.20 | 1.90 | 83 | 360 | |
| 29 | Ex. | 0.740 | 0.120 | 0.090 | 0.050 | 0.000 | 0.000 | 0.000 | amorphous | 1.42 | 2.70 | 0.17 | 5.04 | 2.34 | 87 | 350 | |
| 30 | Ex. | 0.720 | 0.140 | 0.090 | 0.050 | 0.000 | 0.000 | 0.000 | amorphous | 1.38 | 2.70 | 0.17 | 5.09 | 2.39 | 89 | 352 | |
| 31 | Comp. Ex. | 0.710 | 0.150 | 0.090 | 0.050 | 0.000 | 0.000 | 0.000 | amorphous | 1.22 | 2.90 | 0.17 | 5.80 | 2.90 | 100 | 335 | |

TABLE 4

| Example/ Fe(1 – (a + b + c + d + e + f))MaBbPcSidCeSf_XRD | | | | | | | | | Saturation Magnetic Flux | Coer- civity of | Average | Coer- civity of | ΔHc | Coer- civity | | |
|--|-----------------------------|----------------|--------|--------|---------|--------|-----------------------------|--------|---------------------------------|-------------------------|---------------------------|-----------------------|-------------------------|-----------------------|------------|-----|
| Sam- ple No. | Compar- ative Example | M (Nb) a | B b | P c | Si d | C e | Before Heat Treatment | S f | Density of Ribbons Bs (T) | Ribbons Hca (A/m) | Crack Interval (mm) | Core Hcb (A/m) | [Hcb – Hca] (A/m) | Change Rate (%) | Ls (μH) | |
| 34 | Comp. Ex. | 0.870 | 0.060 | 0.020 | 0.050 | 0.000 | 0.000 | 0.000 | crystal | 1.60 | 217 | 0.17 | 438 | 221 | 102 | 7 |
| 35 | Ex. | 0.865 | 0.060 | 0.025 | 0.050 | 0.000 | 0.000 | 0.000 | amorphous | 1.62 | 2.60 | 0.17 | 4.29 | 1.69 | 65 | 351 |
| 36 | Ex. | 0.830 | 0.060 | 0.060 | 0.050 | 0.000 | 0.000 | 0.000 | amorphous | 1.57 | 2.10 | 0.17 | 3.70 | 1.60 | 76 | 363 |
| 37 | Ex. | 0.810 | 0.060 | 0.080 | 0.050 | 0.000 | 0.000 | 0.000 | amorphous | 1.56 | 1.80 | 0.17 | 3.21 | 1.41 | 78 | 371 |
| 45 | Ex. | 0.800 | 0.060 | 0.090 | 0.050 | 0.000 | 0.000 | 0.000 | amorphous | 1.50 | 1.80 | 0.17 | 3.33 | 1.53 | 85 | 370 |
| 38 | Ex. | 0.770 | 0.060 | 0.120 | 0.050 | 0.000 | 0.000 | 0.000 | amorphous | 1.45 | 2.00 | 0.17 | 3.72 | 1.72 | 86 | 366 |
| 39 | Ex. | 0.740 | 0.060 | 0.150 | 0.050 | 0.000 | 0.000 | 0.000 | amorphous | 1.40 | 2.50 | 0.17 | 4.76 | 2.26 | 90 | 358 |
| 40 | Ex. | 0.690 | 0.060 | 0.200 | 0.050 | 0.000 | 0.000 | 0.000 | amorphous | 1.35 | 2.70 | 0.17 | 5.09 | 2.39 | 88 | 353 |
| 41 | Comp. Ex. | 0.680 | 0.060 | 0.210 | 0.050 | 0.000 | 0.000 | 0.000 | amorphous | 1.20 | 2.90 | 0.17 | 5.83 | 2.93 | 101 | 332 |

TABLE 5

| Example/ Sample No. Example | | | | | | | | | Saturation Magnetic Flux | Coer- civity of | Average | Coer- civity of | ΔH_c | Coer- civity | |
|--|-----------|-------|-------|-------|-------|-------|-------|-----------|--------------------------------|-----------------------|---------------------|-----------------------|-------------------|-----------------|----------------|
| Fe(1 - (a + b + c + d + e + f))MaBbPcSidCeSf_XRD | | | | | | | | | | | | | | | |
| Before Heat Treatment | | | | | | | | | Density of Ribbons Bs (T) | Ribbons Hca (A/m) | Crack Interval (mm) | Core Hcb (A/m) | [Hcb - Hca] (A/m) | Change Rate (%) | Ls (μH) |
| M (Nb) | | | | | | | | | | | | | | | |
| a b P c Si d e f | | | | | | | | | | | | | | | |
| 42 | Ex. | 0.850 | 0.060 | 0.090 | 0.000 | 0.000 | 0.000 | amorphous | 1.71 | 4.80 | 0.17 | 8.16 | 3.36 | 70 | 308 |
| 43 | Ex. | 0.840 | 0.060 | 0.090 | 0.010 | 0.000 | 0.000 | amorphous | 1.73 | 4.60 | 0.17 | 7.84 | 3.24 | 70 | 311 |
| 44 | Ex. | 0.820 | 0.060 | 0.090 | 0.030 | 0.000 | 0.000 | amorphous | 1.66 | 4.20 | 0.17 | 7.48 | 3.28 | 78 | 320 |
| 45 | Ex. | 0.800 | 0.060 | 0.090 | 0.050 | 0.000 | 0.000 | amorphous | 1.50 | 1.80 | 0.17 | 3.33 | 1.53 | 85 | 370 |
| 46 | Ex. | 0.770 | 0.060 | 0.090 | 0.080 | 0.000 | 0.000 | amorphous | 1.47 | 2.20 | 0.17 | 3.98 | 1.78 | 81 | 361 |
| 47 | Ex. | 0.750 | 0.060 | 0.090 | 0.100 | 0.000 | 0.000 | amorphous | 1.44 | 2.50 | 0.17 | 4.75 | 2.25 | 90 | 356 |
| 48 | Ex. | 0.700 | 0.060 | 0.090 | 0.150 | 0.000 | 0.000 | amorphous | 1.37 | 2.70 | 0.17 | 5.08 | 2.38 | 88 | 353 |
| 49 | Comp. Ex. | 0.690 | 0.060 | 0.090 | 0.160 | 0.000 | 0.000 | amorphous | 1.28 | 2.80 | 0.17 | 5.78 | 2.98 | 107 | 329 |

TABLE 6

| Example/ Sample No. Example | | | | | | | | | Saturation Magnetic Flux | Coer- civity of | Average | Coer- civity of | ΔH_c | Coer- civity | |
|--|-----------|-------|-------|-------|-------|-------|-----------------------------|---------------------------------|--------------------------------|---------------------------|----------------------|-------------------------|-----------------------|-------------------|-----|
| Fe(1 - (a + b + c + d + e + f))MaBbPcSidCeSf_XRD | | | | | | | | | | | | | | | |
| Compar- ative | M (Nb) | B | P | Si | C | S | Before Heat Treatment | Density of Ribbons Bs (T) | Ribbons Hca (A/m) | Crack Interval (mm) | Core Hcb (A/m) | [Hcb - Hca] (A/m) | Change Rate (%) | Ls (μH) | |
| | Fe | a | b | c | d | e | f | | | | | | | | |
| 45 Ex. | 0.800 | 0.060 | 0.090 | 0.050 | 0.000 | 0.000 | 0.000 | amorphous | 1.50 | 1.80 | 0.17 | 3.33 | 1.53 | 85 | 370 |
| 50 Ex. | 0.799 | 0.060 | 0.090 | 0.050 | 0.000 | 0.001 | 0.000 | amorphous | 1.51 | 1.40 | 0.17 | 2.59 | 1.19 | 85 | 377 |
| 51 Ex. | 0.795 | 0.060 | 0.090 | 0.050 | 0.000 | 0.005 | 0.000 | amorphous | 1.51 | 1.20 | 0.17 | 2.27 | 1.07 | 89 | 384 |

TABLE 6-continued

| | | | | | | | | | Saturation Magnetic Flux | Coer- civity of | Average | Coer- civity of | ΔH_c | Coer- civity | |
|------------------------------|-----------|---|--------|--------|---------|--------|--------|-----------------------------|---------------------------------|-------------------------|---------------------------|-----------------------|-------------------------|-----------------------|-------------------|
| Example/ Compar- ative | | <u>Fe(1 - (a + b + c + d + e + f))MaBbPcSidCeSf</u> XRD | | | | | | | | | | | | | |
| Sam- ple No. | Example | M (Nb) a | B b | P c | Si d | C e | S f | Before Heat Treatment | Density of Ribbons Bs (T) | Ribbons Hca (A/m) | Crack Interval (mm) | Core Hcb (A/m) | [Hcb - Hca] (A/m) | Change Rate (%) | Ls (μH) |
| 52 | Ex. | 0.790 | 0.060 | 0.090 | 0.050 | 0.000 | 0.010 | 0.000 amorphous | 1.50 | 1.50 | 0.17 | 2.66 | 1.16 | 78 | 377 |
| 53 | Ex. | 0.770 | 0.060 | 0.090 | 0.050 | 0.000 | 0.030 | 0.000 amorphous | 1.48 | 1.70 | 0.17 | 3.05 | 1.35 | 79 | 376 |
| 54 | Comp. Ex. | 0.760 | 0.060 | 0.090 | 0.050 | 0.000 | 0.040 | 0.000 amorphous | 1.43 | 3.20 | 0.17 | 6.56 | 3.36 | 105 | 342 |

TABLE 7

| Example/ Fe(1 - (a + b + c + d + e + f))MaBbPcSidCeSf_XRD | | | | | | | | | Saturation Magnetic Flux | Coer- civity of | Average | Coer- civity of | ΔHc | Coer- civity | |
|--|-----------------------------|----------------|--------|--------|---------|--------|--------|-----------------------------|---------------------------------|-------------------------|---------------------------|-----------------------|-------------------------|-----------------------|------------|
| Sam- ple No. | Compar- ative Example | M (Nb) a | B b | P c | Si d | C e | S f | Before Heat Treatment | Density of Ribbons Bs (T) | Ribbons Hca (A/m) | Crack Interval (mm) | Core Hcb (A/m) | [Hcb - Hca] (A/m) | Change Rate (%) | Ls (μH) |
| 45 | Ex. | 0.800 | 0.060 | 0.090 | 0.050 | 0.000 | 0.000 | amorphous | 1.50 | 1.80 | 0.17 | 3.33 | 1.53 | 85 | 370 |
| 55 | Ex. | 0.799 | 0.060 | 0.090 | 0.050 | 0.000 | 0.000 | amorphous | 1.53 | 2.10 | 0.17 | 3.80 | 1.70 | 81 | 368 |
| 56 | Ex. | 0.795 | 0.060 | 0.090 | 0.050 | 0.000 | 0.000 | amorphous | 1.51 | 2.30 | 0.17 | 4.23 | 1.93 | 84 | 364 |
| 57 | Ex. | 0.790 | 0.060 | 0.090 | 0.050 | 0.000 | 0.000 | amorphous | 1.52 | 2.20 | 0.17 | 4.01 | 1.81 | 82 | 364 |
| 58 | Ex. | 0.770 | 0.060 | 0.090 | 0.050 | 0.000 | 0.030 | amorphous | 1.43 | 2.40 | 0.17 | 4.48 | 2.08 | 87 | 356 |
| 59 | Comp. Ex. | 0.760 | 0.060 | 0.090 | 0.050 | 0.000 | 0.040 | crystal | 1.48 | 345 | 0.17 | 724 | 379 | 110 | 3 |

TABLE 8

| Example/ | | Fe(1 - (a + b + c + d + e + f))MaBbPcSidCeSf_XRD | | | | | | | Saturation Magnetic Flux | Coer- civity of | Average | Coer- civity of | ΔHc | Coer- civity | |
|--------------------|-----------------------------|--|--------|--------|---------|--------|--------|-----------------------------|---------------------------------|-------------------------|---------------------------|-----------------------|-------------------------|-----------------------|------------|
| Sam- ple No. | Compar- ative Example | M (Nb) a | B b | P c | Si d | C e | S f | Before Heat Treatment | Density of Ribbons Bs (T) | Ribbons Hca (A/m) | Crack Interval (mm) | Core Hcb (A/m) | [Hcb - Hca] (A/m) | Change Rate (%) | Ls (μH) |
| 45 | Ex. | 0.800 | 0.060 | 0.090 | 0.050 | 0.000 | 0.000 | amorphous | 1.50 | 1.80 | 0.17 | 3.33 | 1.53 | 85 | 370 |
| 60 | Ex. | 0.795 | 0.060 | 0.090 | 0.050 | 0.005 | 0.000 | amorphous | 1.53 | 1.70 | 0.17 | 3.15 | 1.45 | 86 | 370 |
| 61 | Ex. | 0.790 | 0.060 | 0.090 | 0.050 | 0.010 | 0.000 | amorphous | 1.52 | 1.60 | 0.17 | 2.82 | 1.22 | 76 | 377 |
| 62 | Ex. | 0.780 | 0.060 | 0.090 | 0.050 | 0.020 | 0.000 | amorphous | 1.50 | 1.60 | 0.17 | 2.99 | 1.39 | 87 | 372 |
| 63 | Ex. | 0.770 | 0.060 | 0.090 | 0.050 | 0.030 | 0.000 | amorphous | 1.46 | 2.10 | 0.17 | 3.96 | 1.86 | 88 | 367 |
| 64 | Ex. | 0.740 | 0.060 | 0.090 | 0.050 | 0.060 | 0.000 | amorphous | 1.42 | 2.50 | 0.17 | 4.61 | 2.11 | 85 | 358 |
| 65 | Ex. | 0.810 | 0.030 | 0.090 | 0.000 | 0.070 | 0.000 | amorphous | 1.45 | 4.80 | 0.17 | 8.50 | 3.70 | 77 | 327 |
| 66 | Ex. | 0.790 | 0.030 | 0.090 | 0.000 | 0.090 | 0.000 | amorphous | 1.35 | 4.50 | 0.17 | 8.26 | 3.76 | 84 | 330 |
| 67 | Ex. | 0.745 | 0.030 | 0.090 | 0.000 | 0.135 | 0.000 | amorphous | 1.31 | 4.80 | 0.17 | 8.87 | 4.07 | 85 | 330 |
| 68 | Ex. | 0.725 | 0.030 | 0.090 | 0.000 | 0.155 | 0.000 | amorphous | 1.20 | 4.30 | 0.17 | 8.03 | 3.73 | 87 | 329 |
| 69 | Ex. | 0.705 | 0.030 | 0.090 | 0.000 | 0.175 | 0.000 | amorphous | 1.18 | 3.20 | 0.17 | 6.13 | 2.93 | 92 | 336 |

TABLE 9

| Example/ Fe(1 - (a + b + c + d + e + f))MaBbPcSidCeSf_XRD | | | | | | | | | Saturation Magnetic Flux | Coer- civity of | Average | Coer- civity of | ΔHc | Coer- civity | |
|--|-----------------------------|----------------|--------|--------|---------|--------|--------|-----------------------------|---------------------------------|-------------------------|---------------------------|-----------------------|-------------------------|-----------------------|------------|
| Sam- ple No. | Compar- ative Example | M (Nb) a | B b | P c | Si d | C e | S f | Before Heat Treatment | Density of Ribbons Bs (T) | Ribbons Hca (A/m) | Crack Interval (mm) | Core Hcb (A/m) | [Hcb - Hca] (A/m) | Change Rate (%) | Ls (μH) |
| 70a | Ex. | 0.860 | 0.000 | 0.090 | 0.050 | 0.000 | 0.000 | amorphous | 1.75 | 10.90 | 0.17 | 18.20 | 7.30 | 67 | 205 |
| 70 | Ex. | 0.850 | 0.000 | 0.090 | 0.050 | 0.010 | 0.000 | amorphous | 1.74 | 10.80 | 0.17 | 18.16 | 7.36 | 68 | 209 |
| 71 | Ex. | 0.830 | 0.000 | 0.090 | 0.050 | 0.030 | 0.000 | amorphous | 1.73 | 9.50 | 0.17 | 16.57 | 7.07 | 74 | 223 |
| 72 | Ex. | 0.810 | 0.000 | 0.090 | 0.050 | 0.050 | 0.000 | amorphous | 1.70 | 9.30 | 0.17 | 16.58 | 7.28 | 78 | 228 |
| 73 | Ex. | 0.790 | 0.000 | 0.090 | 0.050 | 0.070 | 0.000 | amorphous | 1.66 | 9.20 | 0.17 | 16.69 | 7.49 | 81 | 229 |
| 74 | Ex. | 0.770 | 0.000 | 0.090 | 0.050 | 0.090 | 0.000 | amorphous | 1.64 | 9.40 | 0.17 | 17.29 | 7.89 | 84 | 227 |
| 74a | Ex. | 0.820 | 0.000 | 0.090 | 0.000 | 0.090 | 0.000 | amorphous | 1.73 | 9.50 | 0.17 | 16.70 | 7.20 | 76 | 225 |

TABLE 10

| Example/ Fe(1 – (a + b + c + d + e + f))MaBbPcSidCeSf XRD | | | | | | | | | Saturation Magnetic Flux | Coer- civity of | Average | Coer- civity of | ΔHc | Coer- civity | |
|--|-----------------------------|----------------|--------|--------|---------|--------|--------|-----------------------------|---------------------------------|-------------------------|---------------------------|-----------------------|-------------------------|-----------------------|------------|
| Sam- ple No. | Compar- ative Example | M (Nb) a | B b | P c | Si d | C e | S f | Before Heat Treatment | Density of Ribbons Bs (T) | Ribbons Hca (A/m) | Crack Interval (mm) | Core Hcb (A/m) | [Hcb – Hca] (A/m) | Change Rate (%) | Ls (μH) |
| 75 | Ex. | 0.730 | 0.080 | 0.120 | 0.070 | 0.000 | 0.000 | amorphous | 1.40 | 2.90 | 0.17 | 5.39 | 2.49 | 86 | 350 |
| 45 | Ex. | 0.800 | 0.060 | 0.090 | 0.050 | 0.000 | 0.000 | amorphous | 1.50 | 1.80 | 0.17 | 3.33 | 1.53 | 85 | 370 |
| 76 | Ex. | 0.880 | 0.040 | 0.030 | 0.050 | 0.000 | 0.000 | amorphous | 1.67 | 2.70 | 0.17 | 4.58 | 1.88 | 70 | 354 |
| 77 | Ex. | 0.900 | 0.030 | 0.030 | 0.040 | 0.000 | 0.000 | amorphous | 1.70 | 2.60 | 0.17 | 4.36 | 1.76 | 68 | 354 |

TABLE 11

| Sample | Example/ Comparative | Fe(1 - (a + b + c + d + e + f))MaBbPcSidCeSfXRD (b~f were the same as those of Sample No. 45) Before | | | Saturation Magnetic Flux Density of Ribbons | Coer- civity of Ribbons Hca | Average Crack Interval | Coer- civity of Core Hcb | ΔH_c [Hcb - Hca] | Coer- civity Change Rate | Ls |
|--------|-------------------------|---|-------|-----------|---|---|------------------------------|--------------------------------------|--------------------------------|-----------------------------------|-------------|
| | | MHeat | | | | | | | | | |
| | | Type | a | Treatment | | | | | | | |
| No. | Example | Type | a | Treatment | Bs (T) | (A/m) | (mm) | (A/m) | (A/m) | (%) | (μH) |
| 45 | Ex. | Nb | 0.060 | amorphous | 1.50 | 1.80 | 0.17 | 3.17 | 1.37 | 76 | 371 |
| 78 | Ex. | Hf | 0.060 | amorphous | 1.51 | 1.80 | 0.17 | 3.16 | 1.36 | 76 | 369 |
| 79 | Ex. | Zr | 0.060 | amorphous | 1.52 | 1.70 | 0.17 | 3.08 | 1.38 | 81 | 375 |
| 80 | Ex. | Ta | 0.060 | amorphous | 1.53 | 1.70 | 0.17 | 3.11 | 1.41 | 83 | 378 |
| 81 | Ex. | Mo | 0.060 | amorphous | 1.50 | 2.00 | 0.17 | 3.68 | 1.68 | 84 | 371 |
| 82 | Ex. | W | 0.060 | amorphous | 1.50 | 2.00 | 0.17 | 3.66 | 1.66 | 83 | 379 |
| 83 | Ex. | V | 0.060 | amorphous | 1.51 | 1.90 | 0.17 | 3.40 | 1.50 | 79 | 382 |
| 84 | Ex. | Ti | 0.060 | amorphous | 1.51 | 2.00 | 0.17 | 3.62 | 1.62 | 81 | 380 |
| 85 | Ex. | Nb _{0.5} Hf _{0.5} | 0.060 | amorphous | 1.52 | 1.80 | 0.17 | 3.28 | 1.48 | 82 | 374 |
| 86 | Ex. | Zr _{0.5} Ta _{0.5} | 0.060 | amorphous | 1.53 | 1.90 | 0.17 | 3.51 | 1.61 | 85 | 376 |
| 87 | Ex. | Nb _{0.4} Hf _{0.3} Zr _{0.3} | 0.060 | amorphous | 1.51 | 2.00 | 0.17 | 3.62 | 1.62 | 81 | 380 |

TABLE 12

| Sam- ple No. | Compar- ative Example | Fe(1 - (α + β)) X1αX2β (The type of M and a-f were the same as those of Sample No. 45) XRD | | | | | Saturation Magnetic Flux | Coer- civity of | Average | Coer- civity of | ΔHc | Coer- civity | |
|--------------------|-----------------------------|--|-----------------------------------|------|-----------------------------------|-------------------|--------------------------------|-----------------------|------------------|-----------------------|--------|-----------------|------------|
| | | X1 | | X2 | | Before | Density of | Ribbons | Crack | Core | [Hcb - | Change | |
| | | Type | α{1 - (a + b + c + d + e + f)} | Type | β{1 - (a + b + c + d + e + f)} | Heat Treatment | Ribbons Bs (T) | Hca (A/m) | Interval (mm) | Hcb (A/m) | Hca] | Rate (%) | Ls (μH) |
| 45 | Ex. | — | 0.000 | — | 0.000 | amorphous | 1.50 | 1.80 | 0.17 | 3.33 | 1.53 | 85 | 370 |
| 89 | Ex. | Co | 0.010 | — | 0.000 | amorphous | 1.53 | 2.10 | 0.17 | 3.78 | 1.68 | 80 | 365 |
| 90 | Ex. | Co | 0.100 | — | 0.000 | amorphous | 1.55 | 2.50 | 0.17 | 4.65 | 2.15 | 86 | 359 |
| 91 | Ex. | Co | 0.400 | — | 0.000 | amorphous | 1.60 | 2.90 | 0.17 | 5.50 | 2.60 | 90 | 354 |
| 92 | Ex. | Ni | 0.010 | — | 0.000 | amorphous | 1.51 | 1.80 | 0.17 | 3.19 | 1.39 | 77 | 373 |
| 93 | Ex. | Ni | 0.100 | — | 0.000 | amorphous | 1.47 | 1.70 | 0.17 | 3.10 | 1.40 | 82 | 373 |
| 94 | Ex. | Ni | 0.400 | — | 0.000 | amorphous | 1.42 | 1.60 | 0.17 | 2.76 | 1.16 | 72 | 377 |
| 95 | Ex. | — | 0.000 | Al | 0.001 | amorphous | 1.52 | 1.80 | 0.17 | 3.19 | 1.39 | 77 | 374 |
| 96 | Ex. | — | 0.000 | Al | 0.005 | amorphous | 1.51 | 1.80 | 0.17 | 3.18 | 1.38 | 77 | 371 |
| 97 | Ex. | — | 0.000 | Al | 0.010 | amorphous | 1.51 | 1.70 | 0.17 | 2.97 | 1.27 | 75 | 370 |
| 98 | Ex. | — | 0.000 | Al | 0.030 | amorphous | 1.50 | 1.80 | 0.17 | 3.22 | 1.42 | 79 | 372 |
| 99 | Ex. | — | 0.000 | Zn | 0.001 | amorphous | 1.50 | 1.80 | 0.17 | 3.25 | 1.45 | 81 | 372 |
| 100 | Ex. | — | 0.000 | Zn | 0.005 | amorphous | 1.52 | 1.90 | 0.17 | 3.44 | 1.54 | 81 | 370 |
| 101 | Ex. | — | 0.000 | Zn | 0.010 | amorphous | 1.50 | 1.80 | 0.17 | 3.23 | 1.43 | 79 | 375 |
| 102 | Ex. | — | 0.000 | Zn | 0.030 | amorphous | 1.51 | 1.90 | 0.17 | 3.46 | 1.56 | 82 | 372 |
| 103 | Ex. | — | 0.000 | Sn | 0.001 | amorphous | 1.52 | 1.80 | 0.17 | 3.27 | 1.47 | 82 | 374 |
| 104 | Ex. | — | 0.000 | Sn | 0.005 | amorphous | 1.51 | 1.90 | 0.17 | 3.49 | 1.59 | 84 | 367 |
| 105 | Ex. | — | 0.000 | Sn | 0.010 | amorphous | 1.52 | 1.90 | 0.17 | 3.47 | 1.57 | 83 | 375 |
| 106 | Ex. | — | 0.000 | Sn | 0.030 | amorphous | 1.50 | 2.00 | 0.17 | 3.68 | 1.68 | 84 | 368 |
| 107 | Ex. | — | 0.000 | Cu | 0.001 | amorphous | 1.52 | 1.60 | 0.17 | 2.84 | 1.24 | 77 | 376 |
| 108 | Ex. | — | 0.000 | Cu | 0.005 | amorphous | 1.52 | 1.70 | 0.17 | 3.06 | 1.36 | 80 | 373 |
| 109 | Ex. | — | 0.000 | Cu | 0.010 | amorphous | 1.52 | 1.50 | 0.17 | 2.74 | 1.24 | 83 | 377 |
| 110 | Ex. | — | 0.000 | Cu | 0.030 | amorphous | 1.54 | 1.60 | 0.17 | 2.77 | 1.17 | 73 | 375 |
| 111 | Ex. | — | 0.000 | Cr | 0.001 | amorphous | 1.52 | 1.80 | 0.17 | 3.26 | 1.46 | 81 | 371 |
| 112 | Ex. | — | 0.000 | Cr | 0.005 | amorphous | 1.51 | 1.70 | 0.17 | 3.10 | 1.40 | 82 | 376 |
| 113 | Ex. | — | 0.000 | Cr | 0.010 | amorphous | 1.50 | 1.80 | 0.17 | 3.23 | 1.43 | 79 | 370 |

TABLE 12-continued

| Fe(1 - (α + β)) X1αX2β (The type of M and a-f were the same as those of Sample No. 45) | | | | | | XRD | Saturation Magnetic Flux | Coer- civity of | Average | Coer- civity of | ΔHc | Coer- civity | |
|--|-----------------------------|------|-----------------------------------|------|-----------------------------------|-------------------|--------------------------------|-----------------------|------------------|-----------------------|--------|-----------------|------------|
| Sam- ple No. | Compar- ative Example | X1 | | X2 | | Before | Density of | Ribbons | Crack | Core | [Hcb - | Change | |
| | | Type | α{1 - (a + b + c + d + e + f)} | Type | β{1 - (a + b + c + d + e + f)} | Heat Treatment | Ribbons Bs (T) | Hca (A/m) | Interval (mm) | Hcb (A/m) | Hca] | Rate (%) | LS (μH) |
| 114 | Ex. | — | 0.000 | Cr | 0.030 | amorphous | 1.51 | 1.90 | 0.17 | 3.36 | 1.46 | 77 | 370 |
| 115 | Ex. | — | 0.000 | Bi | 0.001 | amorphous | 1.51 | 1.80 | 0.17 | 3.21 | 1.41 | 78 | 375 |
| 116 | Ex. | — | 0.000 | Bi | 0.005 | amorphous | 1.50 | 1.70 | 0.17 | 3.07 | 1.37 | 80 | 371 |
| 117 | Ex. | — | 0.000 | Bi | 0.010 | amorphous | 1.49 | 1.80 | 0.17 | 3.28 | 1.48 | 82 | 374 |
| 118 | Ex. | — | 0.000 | Bi | 0.030 | amorphous | 1.48 | 2.00 | 0.17 | 3.71 | 1.71 | 85 | 365 |
| 119 | Ex. | — | 0.000 | La | 0.001 | amorphous | 1.52 | 1.80 | 0.17 | 3.23 | 1.43 | 80 | 378 |
| 120 | Ex. | — | 0.000 | La | 0.005 | amorphous | 1.51 | 1.90 | 0.17 | 3.45 | 1.55 | 82 | 370 |
| 121 | Ex. | — | 0.000 | La | 0.010 | amorphous | 1.49 | 2.10 | 0.17 | 3.94 | 1.84 | 88 | 369 |
| 122 | Ex. | — | 0.000 | La | 0.030 | amorphous | 1.48 | 2.10 | 0.17 | 3.85 | 1.75 | 83 | 362 |
| 123 | Ex. | — | 0.000 | Y | 0.001 | amorphous | 1.51 | 1.90 | 0.17 | 3.53 | 1.63 | 86 | 368 |
| 124 | Ex. | — | 0.000 | Y | 0.005 | amorphous | 1.49 | 1.80 | 0.17 | 3.29 | 1.49 | 83 | 370 |
| 125 | Ex. | — | 0.000 | Y | 0.010 | amorphous | 1.48 | 1.80 | 0.17 | 3.22 | 1.42 | 79 | 372 |
| 126 | Ex. | — | 0.000 | Y | 0.030 | amorphous | 1.49 | 2.00 | 0.17 | 3.74 | 1.74 | 87 | 369 |
| 127 | Ex. | — | 0.000 | N | 0.001 | amorphous | 1.49 | 2.00 | 0.17 | 3.60 | 1.60 | 80 | 368 |
| 128 | Ex. | — | 0.000 | O | 0.001 | amorphous | 1.50 | 1.90 | 0.17 | 3.37 | 1.47 | 77 | 369 |
| 129 | Ex. | Co | 0.100 | Al | 0.050 | amorphous | 1.52 | 2.10 | 0.17 | 3.96 | 1.86 | 89 | 368 |
| 130 | Ex. | Co | 0.100 | Zn | 0.050 | amorphous | 1.54 | 2.20 | 0.17 | 4.07 | 1.87 | 85 | 366 |
| 131 | Ex. | Co | 0.100 | Sn | 0.050 | amorphous | 1.53 | 2.20 | 0.17 | 4.07 | 1.87 | 85 | 362 |
| 132 | Ex. | Co | 0.100 | Cu | 0.050 | amorphous | 1.53 | 2.00 | 0.17 | 3.75 | 1.75 | 87 | 372 |
| 133 | Ex. | Co | 0.100 | Cr | 0.050 | amorphous | 1.53 | 2.10 | 0.17 | 3.94 | 1.84 | 87 | 370 |
| 134 | Ex. | Co | 0.100 | Bi | 0.050 | amorphous | 1.51 | 2.20 | 0.17 | 4.08 | 1.88 | 86 | 365 |
| 135 | Ex. | Co | 0.100 | La | 0.050 | amorphous | 1.52 | 2.30 | 0.17 | 4.24 | 1.94 | 85 | 359 |
| 136 | Ex. | Co | 0.100 | Y | 0.050 | amorphous | 1.53 | 2.30 | 0.17 | 4.34 | 2.04 | 89 | 364 |
| 137 | Ex. | Ni | 0.100 | Al | 0.050 | amorphous | 1.48 | 1.70 | 0.17 | 3.06 | 1.36 | 80 | 374 |
| 138 | Ex. | Ni | 0.100 | Zn | 0.050 | amorphous | 1.47 | 1.70 | 0.17 | 3.15 | 1.45 | 85 | 373 |
| 139 | Ex. | Ni | 0.100 | Sn | 0.050 | amorphous | 1.48 | 1.60 | 0.17 | 2.81 | 1.21 | 76 | 373 |
| 140 | Ex. | Ni | 0.100 | Cu | 0.050 | amorphous | 1.49 | 1.60 | 0.17 | 2.79 | 1.19 | 74 | 374 |
| 141 | Ex. | Ni | 0.100 | Cr | 0.050 | amorphous | 1.47 | 1.70 | 0.17 | 2.97 | 1.27 | 75 | 373 |
| 142 | Ex. | Ni | 0.100 | Bi | 0.050 | amorphous | 1.48 | 1.80 | 0.17 | 3.27 | 1.47 | 82 | 370 |
| 143 | Ex. | Ni | 0.100 | La | 0.050 | amorphous | 1.46 | 1.80 | 0.17 | 3.29 | 1.49 | 83 | 369 |
| 144 | Ex. | Ni | 0.100 | Y | 0.050 | amorphous | 1.45 | 1.80 | 0.17 | 3.31 | 1.51 | 84 | 376 |

[0132] In the soft magnetic ribbons of all of the above-mentioned examples, the fine structure was a structure including Fe based nanocrystals, and the Fe based nanocrystals had an average grain size of 5.0 nm or more and 30 nm or less. The examples whose soft magnetic ribbons had a composition falling within the specific range had a favorable coercivity change rate as compared with that of the comparative examples whose soft magnetic ribbons had a composition falling out of the specific range. In Sample 34 (too small B content (b)) and Sample 59 (too large S content (f)), the fine structure of the soft magnetic ribbons before the heat treatment was a crystal structure, Fe based nanocrystals could not be deposited by the heat treatment, and the coercivity was significantly high. In addition, the inductance Ls of the magnetic cores was significantly low.

Experimental Example 3

[0133] Except for changing the temperature of the molten metal obtained by heating the base alloys and further changing the existence of the heat treatment, the heat treatment temperature, and the heat treatment time, Experimental Example 3 was carried out with the same conditions as Sample No. 45 of Experimental Example 2. The results are shown in Table 13 and Table 14. In examples and comparative examples of Table 13 not subjected to the heat treatment, for the sake of convenience, the crystal average particle size and the fine structure before the heat treatment were the same as those after the heat treatment.

TABLE 13

| Fe(1 - (a + b + c + d + e + f))MaBbPcSidCeSf (a-f were the same as those of Sample No. 45) | | | | | | | | | | | |
|--|---|--|------------------------------------|---|---|--|----------------------------------|---|--|---|---------------------------------------|
| Sam- ple No. | Example/ Compar- ative Example | Temperature for Manu- facturing Ribbons (° C.) | XRD Before Heat Treatment | Crystal Average | | Heat Treatment Temperature (° C.) | Heat Treatment Time (h) | Crystal Average | | Saturation Magnetic Flux Density of Ribbons Bs (T) | Coer- civity of Hca (A/m) |
| | | | | Particle Size Before Heat Treatment (nm) | Fine Structure Before Heat Treatment | | | Grain Size After Heat Treatment (nm) | Fine Structure After Heat Treatment | | |
| 145 | Comp. Ex. | 1200 | amorphous | no fine crystals | amorphous | no heat treatment | | no fine crystals | amorphous | 0.70 | 8.90 |
| 146 | Ex. | 1225 | amorphous | 0.1 | nanohetero | no heat treatment | | 0.1 | nanohetero | 1.21 | 10.10 |
| 147 | Ex. | 1250 | amorphous | 0.3 | nanohetero | no heat treatment | | 0.3 | nanohetero | 1.25 | 9.70 |

TABLE 13-continued

| Fe(1 - (a + b + c + d + e + f))MaBbPcSidCeSf (a-f were the same as those of Sample No. 45) | | | | | | | | | | | |
|--|-----------------------------|--|---------------------------|--|--------------------------------------|-----------------------------------|-------------------------|--|-------------------------------------|--|-------------------------|
| Sample No. | Example/Comparative Example | Temperature for Manufacturing Ribbons (° C.) | XRD Before Heat Treatment | Crystal Average Particle Size Before Heat Treatment (nm) | Fine Structure Before Heat Treatment | Heat Treatment Temperature (° C.) | Heat Treatment Time (h) | Crystal Average Grain Size After Heat Treatment (nm) | Fine Structure After Heat Treatment | Saturation Magnetic Flux Density of Ribbons Bs (T) | Coercivity of Hca (A/m) |
| 148 | Ex. | 1250 | amorphous | 0.3 | nanohetero | no heat treatment | | 0.3 | nanohetero | 1.25 | 9.70 |
| 149 | Ex. | 1250 | amorphous | 0.3 | nanohetero | no heat treatment | | 0.3 | nanohetero | 1.25 | 9.70 |
| 150 | Ex. | 1250 | amorphous | 0.3 | nanohetero | no heat treatment | | 0.3 | nanohetero | 1.25 | 9.70 |
| 151 | Ex. | 1275 | amorphous | 10 | nanohetero | no heat treatment | | 10 | nanohetero | 1.31 | 8.50 |
| 152 | Ex. | 1275 | amorphous | 10 | nanohetero | no heat treatment | | 10 | nanohetero | 1.31 | 8.50 |
| 153 | Ex. | 1300 | amorphous | 15 | nanohetero | no heat treatment | | 15 | nanohetero | 1.32 | 7.80 |
| 154 | Ex. | 1300 | amorphous | 15 | nanohetero | no heat treatment | | 15 | nanohetero | 1.32 | 7.80 |
| 155 | Ex. | 1200 | amorphous | no fine crystals | amorphous | 600 | 1 | 10 | nanohetero | 1.45 | 2.00 |
| 156 | Ex. | 1225 | amorphous | 0.1 | nanohetero | 450 | 1 | 3 | nanohetero | 1.48 | 2.00 |
| 157 | Ex. | 1250 | amorphous | 0.3 | nanohetero | 500 | 1 | 5 | nanohetero | 1.50 | 1.90 |
| 158 | Ex. | 1250 | amorphous | 0.3 | nanohetero | 550 | 1 | 10 | Fe based nanocrystal | 1.50 | 1.80 |
| 159 | Ex. | 1250 | amorphous | 0.3 | nanohetero | 575 | 1 | 13 | Fe based nanocrystal | 1.51 | 1.70 |
| 160 | Ex. | 1250 | amorphous | 0.3 | nanohetero | 600 | 1 | 10 | Fe based nanocrystal | 1.52 | 1.80 |
| 161 | Ex. | 1275 | amorphous | 10 | nanohetero | 600 | 1 | 12 | Fe based nanocrystal | 1.52 | 1.90 |
| 162 | Ex. | 1275 | amorphous | 10 | nanohetero | 650 | 1 | 30 | Fe based nanocrystal | 1.52 | 1.90 |
| 163 | Ex. | 1300 | amorphous | 15 | nanohetero | 600 | 1 | 17 | Fe based nanocrystal | 1.51 | 2.30 |
| 164 | Ex. | 1300 | amorphous | 15 | nanohetero | 650 | 10 | 50 | Fe based nanocrystal | 1.43 | 2.90 |

TABLE 14

| Sample No. | Example/Comparative Example | Fragmentation | Average Crack Interval (mm) | Punching Possibility | Coercivity of Core Hcb (A/m) | ΔH_c [Hcb - Hca] (A/m) | Coercivity Change Rate (%) | Ls (μ H) |
|------------|-----------------------------|---------------|-----------------------------|----------------------|------------------------------|--------------------------------|----------------------------|---------------|
| 145 | Comp. Ex. | impossible | — | impossible | — | — | — | — |
| 146 | Ex. | yes | 0.17 | possible | 18.93 | 8.83 | 87 | 231 |
| 147 | Ex. | yes | 0.17 | possible | 17.61 | 7.91 | 82 | 241 |
| 148 | Ex. | yes | 0.17 | possible | 17.76 | 8.06 | 83 | 237 |
| 149 | Ex. | yes | 0.17 | possible | 17.71 | 8.01 | 83 | 237 |
| 150 | Ex. | yes | 0.17 | possible | 17.71 | 8.01 | 83 | 241 |
| 151 | Ex. | yes | 0.17 | possible | 15.21 | 6.71 | 79 | 249 |
| 152 | Ex. | yes | 0.17 | possible | 14.87 | 6.37 | 75 | 252 |
| 153 | Ex. | yes | 0.17 | possible | 14.56 | 6.76 | 87 | 254 |
| 154 | Ex. | yes | 0.17 | possible | 14.65 | 6.85 | 88 | 248 |
| 155 | Ex. | yes | 0.17 | possible | 3.53 | 1.53 | 77 | 360 |
| 156 | Ex. | yes | 0.17 | possible | 3.54 | 1.54 | 77 | 367 |
| 157 | Ex. | yes | 0.17 | possible | 3.48 | 1.58 | 83 | 370 |
| 158 | Ex. | yes | 0.17 | possible | 3.23 | 1.43 | 79 | 371 |
| 159 | Ex. | yes | 0.17 | possible | 3.01 | 1.31 | 77 | 372 |
| 160 | Ex. | yes | 0.17 | possible | 3.27 | 1.47 | 82 | 371 |
| 161 | Ex. | yes | 0.17 | possible | 3.36 | 1.46 | 77 | 375 |
| 162 | Ex. | yes | 0.17 | possible | 3.53 | 1.63 | 86 | 374 |
| 163 | Ex. | yes | 0.17 | possible | 4.09 | 1.79 | 78 | 350 |
| 164 | Ex. | yes | 0.17 | possible | 5.38 | 2.48 | 86 | 328 |

[0134] According to Table 13 and Table 14, even if the temperature of the molten metal obtained by heating the base alloys was changed, and the existence of heat treatment, the heat treatment temperature, and the heat treatment time were further changed, when the fine structure of the soft magnetic ribbons finally used was a nanohetero structure or a structure including Fe based nanocrystals, the soft magnetic ribbons were able to be fragmented and punched, and the coercivity change rate was favorable. On the other hand,

when the fine structure of the soft magnetic ribbons finally used was an amorphous structure, the soft magnetic ribbons could not be fragmented or punched out.

Experimental Example 4

[0135] Except for changing the space factor of the magnetic material, Experimental Example 4 was carried out with the same conditions as Sample No. 7 of Experimental Example 1. The results are shown in Table 15 and Table 16.

TABLE 15

| Sample No. | Example/Comparative Example | Composition | XRD Before Heat Treatment | Heat Treatment | Fine Structure After Heat Treatment | Saturation Magnetic Flux Density of Ribbons Bs (T) | Coercivity of Ribbons Hca (A/m) |
|------------|-----------------------------|---|---------------------------|----------------|-------------------------------------|--|---------------------------------|
| 7 | Ex. | Fe _{0.735} Nb _{0.03} B _{0.09} Si _{0.135} Cu _{0.01} | amorphous | yes | Fe based nanocrystal | 1.21 | 0.5 |
| 165 | Ex. | Fe _{0.735} Nb _{0.03} B _{0.09} Si _{0.135} Cu _{0.01} | amorphous | yes | Fe based nanocrystal | 1.21 | 0.5 |
| 166 | Ex. | Fe _{0.735} Nb _{0.03} B _{0.09} Si _{0.135} Cu _{0.01} | amorphous | yes | Fe based nanocrystal | 1.21 | 0.5 |

TABLE 16

| Sample No. | Example/Comparative Example | Fragmentation | Average Crack Interval (mm) | Punching Possibility | Space Factor | Coercivity of Core Hcb (A/m) | ΔH_c [Hcb - Hca] (A/m) | Coercivity Change Rate (%) | Ls (μ H) |
|------------|-----------------------------|---------------|-----------------------------|----------------------|--------------|------------------------------|--------------------------------|----------------------------|---------------|
| 7 | Ex. | yes | 0.17 | possible | 85% | 0.86 | 0.36 | 72 | 356 |
| 165 | Ex. | yes | 0.17 | possible | 96% | 0.87 | 0.37 | 74 | 361 |
| 166 | Ex. | yes | 0.17 | possible | 72% | 0.85 | 0.35 | 70 | 271 |

[0136] According to Table 15 and Table 16, even if the space factor was changed, the coercivity change rate was favorable in examples having a space factor of 70% or more and 99.5% or less. Incidentally, the higher the space factor was, the higher the inductance Ls tended to be, and the larger the coercivity change rate tended to be.

NUMERICAL REFERENCES

[0137] 10 . . . magnetic core

[0138] 12 . . . soft magnetic layer

[0139] 13 . . . protective film

[0140] 14 . . . adhesive layer

[0141] A . . . center plane

[0142] B . . . virtual line

[0143] C . . . crack

[0144] D . . . intersection

1-13. (canceled)

14. A magnetic core comprising laminated soft magnetic layers having cracks, wherein

the soft magnetic layers include Fe as a main component, the soft magnetic layers have a composition formula of

$(Fe_{(1-(\alpha+\beta))}X_1X_2)_{(1-(a+b+c+d+e+f))}M_dB_bP_cSi_dC_eS_f$ in which X1 is one or more selected from a group consisting of Co and Ni, X2 is one or more selected from a group consisting of Al, Mn, Ag, Zn, Sn, As, Sb, Cu, Cr, Bi, N, O, and rare earth elements, and M is one or more selected from a group consisting of Nb, Hf, Zr, Ta, Mo, V, and W,

$0 \leq a \leq 0.140$, $0.020 < b \leq 0.200$, $0 \leq c \leq 0.150$, $0 \leq d \leq 0.180$, $0 \leq e < 0.040$, $0 \leq f \leq 0.030$, $\alpha \geq 0$, $\beta \geq 0$, and $0 \leq a + \beta \leq 0.50$ are satisfied,

one or more of a, c, and d are larger than zero, and a nanohetero structure including an amorphous phase and fine crystals existing in the amorphous phase is observed in the soft magnetic layers.

15. The magnetic core according to claim 14, wherein the fine crystals have an average grain size of 0.3-5 nm.

16. A magnetic core comprising laminated soft magnetic layers having cracks, wherein

the soft magnetic layers include Fe as a main component, the soft magnetic layers have a composition formula of

$(Fe_{(1-(\alpha+\beta))}X_1X_2)_{(1-(a+b+c+d+e+f))}M_dB_bP_cSi_dC_eS_f$ where X1 is one or more selected from a group con-

sisting of Co and Ni, X2 is one or more selected from a group consisting of Al, Mn, Ag, Zn, Sn, As, Sb, Cu, Cr, Bi, N, O, and rare earth elements, and M is one or more selected from a group consisting of Nb, Hf, Zr, Ta, Mo, V, and W,

$0 \leq a \leq 0.140$, $0.020 < b \leq 0.200$, $0 \leq c \leq 0.150$, $0 \leq d \leq 0.180$, $0 \leq e < 0.040$, $0 \leq f \leq 0.030$, $\alpha \geq 0$, $\beta \geq 0$, and $0 \leq a + \beta \leq 0.50$ are satisfied,

one or more of a, c, and d are larger than zero, and a structure including Fe based nanocrystals is observed in the soft magnetic layers.

17. The magnetic core according to claim 16, wherein the Fe based nanocrystals have an average grain size of 5-30 nm.

18. The magnetic core according to claim 14, wherein the soft magnetic layers are fragmented so as to have an average crack interval of 0.015 mm or more and 1.0 mm or less.

19. The magnetic core according to claim 16, wherein the soft magnetic layers are fragmented so as to have an average crack interval of 0.015 mm or more and 1.0 mm or less.

20. The magnetic core according to claim 14, wherein a space factor of a magnetic material of the magnetic core is 70.0% or more and 99.5% or less.

21. The magnetic core according to claim 16, wherein a space factor of a magnetic material of the magnetic core is 70.0% or more and 99.5% or less.

22. The magnetic core according to claim 14, wherein $0.020 \leq a \leq 0.100$ is satisfied.

23. The magnetic core according to claim 16, wherein $0.020 \leq a \leq 0.100$ is satisfied.

24. The magnetic core according to claim 14, wherein $0.050 \leq a \leq 0.80$ is satisfied.

25. The magnetic core according to claim 16, wherein $0.050 \leq a \leq 0.80$ is satisfied.

26. The magnetic core according to claim 14, wherein $0.730 \leq 1-(a+b+c+d+e+f) \leq 0.950$ is satisfied.

27. The magnetic core according to claim 16, wherein $0.730 \leq 1-(a+b+c+d+e+f) \leq 0.950$ is satisfied.

28. The magnetic core according to claim 14, wherein $\alpha=0$ is satisfied.

29. The magnetic core according to claim 16, wherein $\alpha=0$ is satisfied.

30. The magnetic core according to claim **14**, wherein $\beta=0$ is satisfied.

31. The magnetic core according to claim **16**, wherein $\beta=0$ is satisfied.

32. A coil device comprising the magnetic core according to claim **14** and a coil.

33. A coil device comprising the magnetic core according to claim **16** and a coil.

34. A method of manufacturing a magnetic core, comprising the steps of:

fragmenting each of a plurality of soft magnetic ribbons,
and

laminating the fragmented soft magnetic ribbons in a thickness direction.

* * * * *